CONTENTS G THROUGH M

THE ABUNDANCE OF ^{26}AL IN PLANETARY SYSTEMS: DOES IT VARY, AND DOES IT MATTER?. Eric Gaidos[1], Nicholas Moskovitz[2,3], Daniel Rogers[3], Jonathan Williams[2], [1]*Department of Geology & Geophysics,* [2]*Institute for Astronomy,* [3]*Department of Physics & Astronomy, University of Hawaii at Manoa, Honolulu HI 96822, USA, (gaidos@hawaii.edu).*

Primitive meteorites contain compelling evidence for the presence of short-lived radionuclides (SLRs) early in Solar System history. Although both internal and external sources may have contributed to SLR abundances, one or more nearby massive stars was likely to be the source of ^{60}Fe ($\tau_{1/2}$ = 1.5 Myr) and at least some of the ^{26}Al ($\tau_{1/2}$ = 0.72 Myr) [1]. The latter isotope is the principal radiogenic heat source implicated in the early melting and differentiation of meteorite parent bodies [2]. The statistics of such an association strongly points to the origin of the Sun in a dense stellar cluster [3] that probably dispersed after 1-10 Myr, an inference consistent with recent infrared surveys that such clusters are the site of $\sim$90% of all star formation in the Galaxy [4].

Besides SLRs, the influence of an early cluster environment on the Solar System (and most other planetary systems) could include stronger gravitational tides [5], more frequent perturbations by passing stars [6], and an enhanced UV radiation field [7]. Moreover, the stochastic nature of trajectories of individual stars within any given cluster (as well as from cluster to cluster) means that the environments experienced by individual stars may vary greatly. Mass segregation within clusters, if it occurs, could also impose trends with stellar mass.

We are investigating variations in the environment of cluster stars using simulations of open stellar clusters with the NBODY4 dynamical code [8] running on the Cambridge University GRAPE-6a parallel architecture supercomputer card [9]. NBODY4 uses the Hermite scheme of dynamical integration; close two-body enounters are handled using the Kustaanheimo-Stiefel regularization method and multiple systems are treated by chain regularization. Stellar evolution is incorporated in the NBODY4 code, including mass loss in winds and supernova events.

Figure 1 plots the trajectories (radius from the cluster center vs. time) for five solar-mass stars selected from a simulation of a 1000-star cluster. Initial conditions are randomized locations within a Plummer sphere, and a Salpeter IMF with mean stellar mass of $0.5 M_\odot$ is assumed. The virial ratio is set to 1.0 to emulate the effect of instantaneous loss of 50% of cluster mass (as gas) during star formation [10]. Variation in distance from the cluster center (the likely location for the most massive members of the cluster and the presumed source of ^{26}Al) will result in different abundances in the planetary systems around these stars. We capture this variation by integrating an exposure quantity

$$e = \int_0^\infty r^{-2} e^{-t/\tau_{1/2}} dt, \qquad (1)$$

which includes the effect of isotope decay. This quantity e is the integrated fluence from a decaying point source at the cluster center; it is used here for the basis of measuring variation rather than for direct interpretation. Figure 2 shows that e varies by as much as 10^3 between stars.

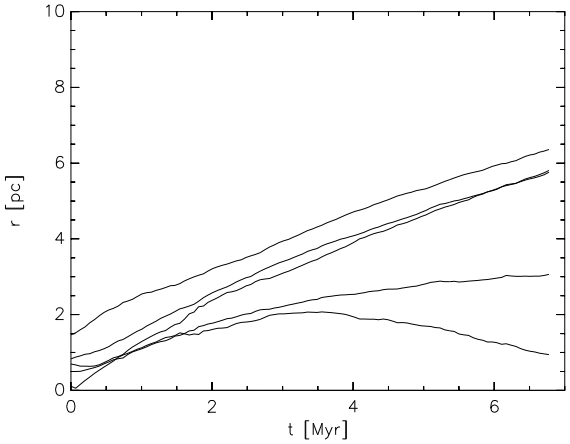

Figure 1: Diverging trajectories (distance from cluster center vs. time) of five solar-mass stars in a 1000-star cluster simulation.

The importance of ^{26}Al as a heat source in the early Solar System is now widely accepted and is underscored by evidence for differentiation of some meteorite parent bodies prior to chondrule formation (i.e., <3 Myr after CAI formation) [11,12]. Several models describing the thermal and petrological evolution of asteroids and meteorite parent bodies include this heat source [13,14,15]. However, the effect of ^{26}Al heating and early thermal evolution on planet formation itself has not been investigated. The rough equality between the time scale for growth of embryos at 1 AU ($\sim$1 Myr [16]) and the period of maximum heating by ^{26}Al suggests that any effect might be particularly pronounced in the terrestrial planet region. Nevertheless, the requirement that Jupiter's core grow to at least a few $M_\oplus$ before the dissipation of nebular gas in a few Myr [17] means that a role for heating by ^{26}Al (or the longer-lived ^{60}Fe) in outer planet formation cannot be excluded.

Taking a specific heating rate h of 10^7 J Myr^{-1} kg^{-1} [13], a thermal diffusivity of 10^{-6} m^{2}sec^{-1}, and a heat capacity of 10^3 J kg^{-1} K^{-1}, then at times $t_{Myr} \ll 0.72$, the interior temperatures of bodies with $r \geq 6\sqrt{t_{Myr}}$ will be approximately 10^4 K t_{Myr}. Thus, bodies only a few km across can reach the solidus of the Fe-S (1200 K) and silicate (1500 K) systems in ~ 0.15 Myr. Even if planetesimals were initially smaller than this, runaway accretion would have produced bodies of this size within 10^4 yr at 1 AU distances. An input of 10^6 J kg^{-1} into material with a latent heat of fusion of 3×10^5 J kg^{-1} would produce a substantial melt fraction.

The above assumes heat transport by conduction only. The onset of convection in a solid body is governed by the Rayleigh number,

$$Ra \approx \frac{4\alpha\rho^2 G h r^6}{k\kappa\nu}, \qquad (2)$$

where α is the thermal expansion coefficient, ρ is the density, k is the thermal conductivity, and ν is the temperature-dependent specific viscosity. Because of the expected absence of water in the terrestrial planet regime, the viscosities will be much higher than that of Earth's mantle (10^{21} poise) and due to this and the small size, Rayleigh numbers will be well below the critical value of $\sim$1100 required for the onset of convection until temperatures pass the solidus and viscosities fall to about 10^{10} poise. However, the extreme temperature contrast between the surface and the interior under these conditions pushes the critical Ra to a higher value and convection will occur only in a stagnant lid regime, if at all [18]. Small, hot planetesimals are likely to retain stagnant, partially molten interiors and cool surfaces.

Close passage of two "hot" planetesimals of mass m with periapsis q will result in tidal dissipation of an amount of energy ΔE;

$$\Delta E \sim Gm\frac{r^5}{q^6}\frac{k_2}{Q}, \quad (3)$$

where k_2 is the Love number and Q is the quality factor of dissipation [19]. For partially molten bodies, both k_2 and Q will be of order unity and captures will take place if

$$q \leq \left(\frac{Gmr^5}{v^2}\right)^{1/6}, \quad (4)$$

where v is the RMS velocity. During the runaway accretion that precedes oligarchic growth, relative planetesimal velocities will be low and tidal capture more efficient: Nevertheless, because of the weak dependence on v, q is unlikely to be significantly larger than a few times r.

Planetary embyros can suffer viscous disruption during close encounters if their bulk visocity is less than a critical value [20]

$$\eta < \frac{\sqrt{G\rho}\rho r^2}{\epsilon_c}, \quad (5)$$

where the disruptive strain $\epsilon_c \sim 10$. This is roughly 10^8 poise for a 10-km object. Magma viscosities vary considerably with chemistry and water content, but range from 10^3 poise for basaltic magmas up to 10^8 poise for rhyolites. We conclude that partially molten planetesimals are subject to disruption by close encounters with other planetesimals (note that Eqn. 5 is independent of planetesimal mass). Fragmentation produces smaller particles with shorter gas drag damping times that are more easily accreted by growing embryos. Chambers [16] showed that fragmentation (albeit by collisions) can dramatically accelerate oligarch growth. (Leinhardt & Richardson [21] found no effect of fragmentation on accretion rates, but their simulations were gas-free). Likewise, fragments will also experience faster inward drift due to force exerted by the non-Keplerian motion of the gas. In the terrestrial planet region, drift can enhance embryo mass by a factor of a few [16].

Enhanced tidal capture and fragmentation of planetesimals could accelerate growth of oligarchs and increase final embryo masses in ^{26}Al-rich systems. However, the effect on the final giant impact phase is not clear. In the terrestrial planet region, the latter is 1-2 orders of magnitude longer than the former and is thus the rate-limiting step. Stronger perturbations between fewer, more massive embryos may change the elapsed time before orbits begin to cross and merging impacts occur. Whether this alters the ultimate outcome of planetary masses and orbits remains to be studied.

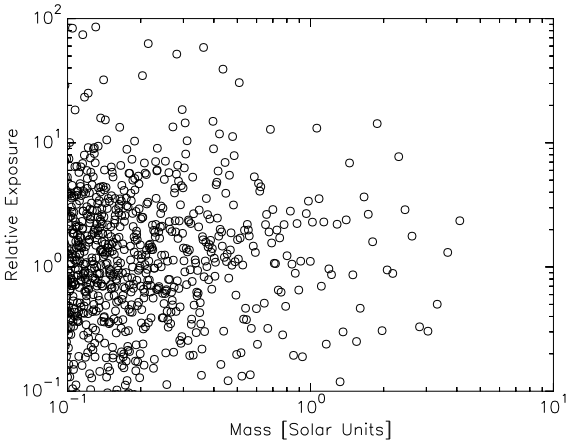

Figure 2: Time-integrated "exposure" (see text for definition) of stars vs. mass.

References: [1] Goswami, J. N. et al., in *Chondrites and the Protoplanetary Disk*, ASP Conf. Ser. 341, 2005, A. N. Krot et al., eds. [2] Ghosh, A., et al., 2006, in *Protostars and Planets V*, B. Reipurth et al., eds., Univ. Arizona Press, Tucson [3] Looney, L. W. et al., *Astrophys. J.*, in press [4] Lada, C. J., & Lada, E. A., 2003, *Annu. Rev. Astron. Asrophys.* 41, 57. [5] Gaidos, E. J., 1995, *Icarus* 114, 258. [6] Fernández, J. A., & Brunini, A., 2000, *Icarus* 145, 580. [7] Adams, F. C., et al., 2006, *Astrophys. J.* 641, 504. [8] Aarseth, S., 2003, *Gravitational N-body Simulations, Tools, and Algorithms*, Cambridge U. Press. [9] Johnson, V., & Arseth, S., 2006, in *Astronomical Data Analysis Software and Systems XV*, ASP Conf. Ser. 351, 165. [10] Bastian, N., & Goodwin, S. P., 2005, *Mon. Not. R. Astron. Soc.* 369, L9. [11] Baker, J., et al., 2005, Nature 436, 1127. [12] Bizzaro, M. et al., 2005, *Astrophys. J.* 632, L41. [13] Ghosh, A., & McSween, H. Y., 1998, *Icarus* 134, 187. [14] Ghosh, A. et al., 2003, *Meteorit. Planet. Sci.* 38, 711. [15] Travis, B. J., & Schubert, G., 2005, *Earth Planet. Sci. Lett.* 240, 234. [16] Chambers, J., 2006, *Icarus* 180, 496. [17] Lissauer, J. J., & Stevenson, D. J., 2006, in *Protostars & Planets V*, B. Reipurth et al., Univ. Arizona Press, Tucson [18] Solomatov, V. S., 1995, *Phys. Fluids* 7, 266. [19] Goldreich, P., 1963, *Mon. Not. R. Astron. Soc.* 126, 257. [20] Asphaug, E. et al., 2006, *Nature* 439, 155. [21] Leinhardt, Z. M., & Richardson, D. C., 2005, *Astrophys. J.* 625, 427.

Acknowledgements: E. G. is supported by NASA grants NNG04GL48G (Terrestrial Planet Finder Foundation Science) and NNA04CC08A (Astrobiology); N. M. is supported by a NASA Graduate Student Research Fellowship; and D. R. is a UH/NASA Space Grant awardee.

REDOX CONTROL ON SULFUR ABUNDANCE AMONG TERRESTRIAL PLANETS

F. Gaillard, B. Scaillet (Institut des Sciences de la Terre d'Orléans (ISTO) UMR6113 CNRS/Université Orléans 1A, rue de la Férollerie 45071 Orléans Cedex 2, France).

Introduction: Sulfur constitutes several wt% of chondrite meteorites, the accretion material of terrestrial planets. It is thought that the high temperature reached during accretion on terrestrial bodies is responsible for substantial volatilization and estimations of sulfur abundance on Earth place a maximum at 0.6wt% [1]. Although classified as a volatile element, sulfur has a significant solubility at high temperature in both molten Fe-metal and silicates [2,3], which dominantly depends on the prevailing redox conditions. Redox conditions of planetary bodies during accretion seem extremely heterogeneous as revealed by variable proportions of iron in the metal (Fe) and oxidized (FeO) forms preserved in meteorites and terrestrial planets. Meteorites collections display completely metallic to completely oxidized samples, which probably make of the redox potential, expressed hereafter as oxygen fugacity, the most variable chemical parameter in the primitive solar system (6 log units of variation in fO2).

Computation and Results: We have calculated the sulfur distribution between molten silicate and metal as a function of oxygen fugacity based on available thermodynamic models [3,4]. We fixed the initial composition of the system in terms of major elements including constant Fe and S contents. We simply allow changes in the ratio of metal over silicate, by simulating variable fO2 conditions. Increasing fO2 decreases sulfur solubility in molten silicate because sulfur and oxygen anions compete for a single anionic site in the melt structure. However, at metal-Fe saturation, increasing fO2 increases FeO content in the silicate, which increases the sulfur solubility in the silicate. This results in rather complex and non-monotonic trends in sulfur partitioning between metal and silicate as fO2 changes (Figure 1). At very reducing fO2, typically prevailing in Enstatite chondrite/achondrite and probably during Mercury's accretion, nearly all sulfur partitions into the silicate portion. Sulfur content in the range 0.1-1 wt% dissolves in the silicate magma ocean consistent with recent measurments on Aubrites basalt [5]. Under relatively oxidized conditions of accretion, probably prevailing in carbonaceous chondrites and on Vesta and Mars, sulfur also strongly partitions in the silicate with concentration in the range 0.08-0.1wt%. In contrast, at intermediate fO2 conditions of accretion such as on Earth, sulfur content in the silicate portion shows a minimum vs. a maximum in S content in the metal. Therefore, accretion of materials homogeneous in S content but differing in their redox state reproduce the high sulfur content in Mars mantle, which exceed the S content in Earth mantle by a factor of 3-4. The volcanic gases therefore emitted on Mars were much more sulfur-rich than on Earth, which must have played a critical role on the development of life on Mars.

Conclusion: Redox variations during accretion on terrestrial planets controlled the metal proportion and rules elements partitioning between metal and silicate. Important differences in measured abundances of sulfur in silicate portion from various terrestrial materials seem to be essentially controlled by redox conditions.

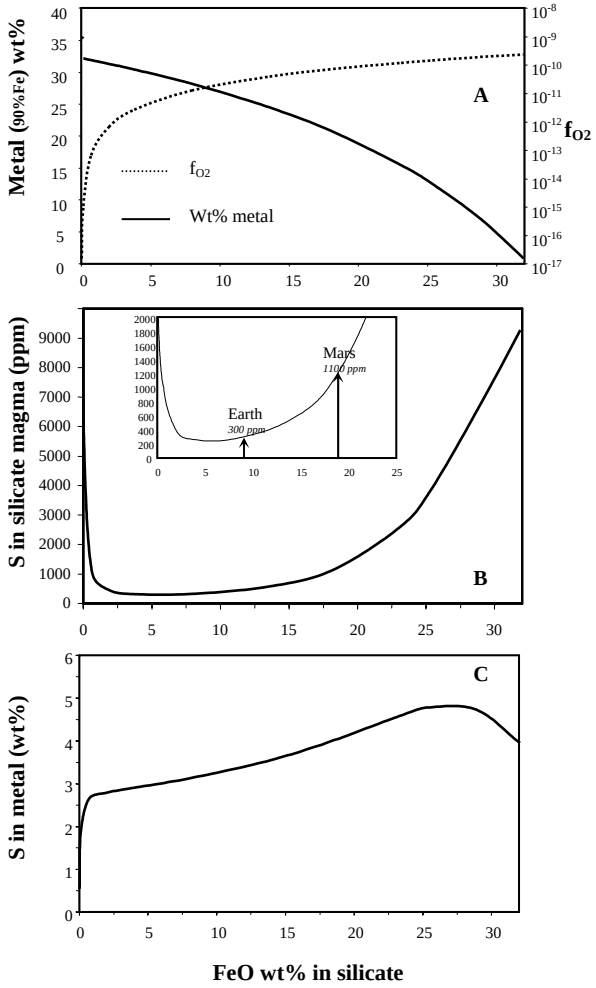

Figure 1: As a function of FeO in the silicate in equilibrium with Fe-metal are shown: A: changes in fO2 and and proportion of metal; B: changes in sulfur content in the silicate; C: changes in sulfur content in the metal. Calculation are performed at 1600°C, 1 atm for a bulk S content at 0.6wt%.

References: [1] Dreibus G. and Palme H. (1996) *Geochim. Cosmochim. Acta, 60,* 1125–1130. [2] Chabot N.L. (2004) *Geochim. Cosmochim. Acta., 68,* 3607-3618. [3] O'Neill H.St. and Mavrogenes J.A. (2002) *Jour. Petrol.,* 43, 1049-1087. [4] Wang et al. (1991) *ISIJ,* 31, 1292-1299. [5] Fogel R.A. (2005) *Geochim. Cosmochim. Acta.* 69, 1633-1648.

ON THE POSSIBLITY OF IMPACT-INDUCED CHEMICAL DIFFERENTIATION OF TERRESTRIAL PLANETS DURING THEIR ACCRETION. M. V. Gerasimov[1], Yu. P. Dikov[1,2], O. I. Yakovlev[1,3]. [1]Space Research Institute, RAS, Profsoyuznaya, 84/32, Moscow, 117997, Russia, mgerasim@mx.iki.rssi.ru; [2]Institute of Ore Deposits, Petrography, Mineralogy and Geochemistry, RAS, Staromonetny per.,35, Moscow, 109017, Russia, dikov@igem.ru; [3]Vernadsky Institute of Geochemistry and Analytical Chemistry, RAS, Kosygin St., 19, Moscow, 119991, Russia, yakovlev@geokhi.ru.

Introduction: The concept of the origin of the Earth and of other earth group planets and satellites by accumulation of large (up to asteroid size) solid bodies implies that nearly every particle of the planet have passed processing in an impact. Most of planetary material has passed multiple processing by successive impacts. The global result of such processing is not yet well understood.

Chemical differentiation during a hypervelocity impact occurs as a planetary local effect, which is limited to only central portion of highly heated collided material. High-temperature processing results in production of chemically different compositions from admittedly initially homogeneous colliding materials. The global planetary effect of multiple impacts during an accretion is a matter of discussion. Generally, one can expect the absence of any globally significant differentiation, but mixing of locally differentiated materials, which restores average composition of planetesimals. Formation of primordial atmosphere and possibly hydrosphere by impact-induced degassing [1,2] is an example of global planetary differentiation for elements with high volatility. The mechanism here is the phase separation of solids and newly formed gases with accumulation of the last in the atmosphere. The question arises whether the volatility of elements can be a reason of their redistribution in the solid material along the radius of a forming planet.

In the present paper we discuss the possible consequences of impact accumulation scenario based on experimental investigation of impact vaporization chemistry.

Differentiation of silicates during an impact: The main mechanism of chemical differentiation of silicates during an impact is the separation of elements between melt and vapor phases. The reason of chemical differentiation here is the selective character of volatility of rock-forming elements, which can result in sufficiently different compositions of impact products (melted residua and vaporized/condensed materials). Behavior of siliceous systems at temperatures 3000 to 5000 K have some peculiarities [3], among which the most pronounced are the volatilization of elements as complex molecular clusters and sufficient temperature driven reduction of iron and of other siderophile elements.

Major elements behavior. Experiments on hypervelocity gas-gum and laser pulse techniques show that

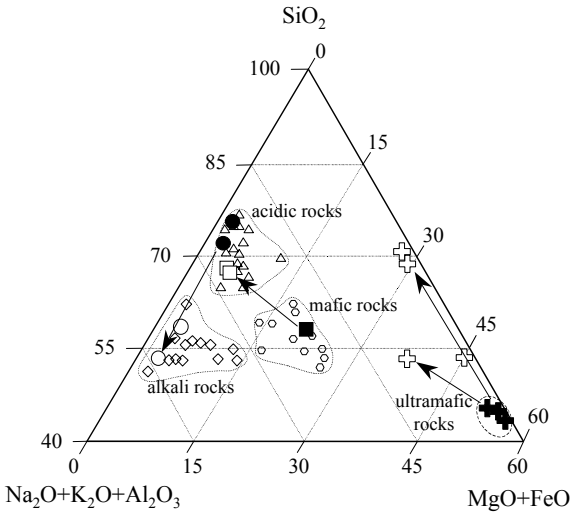

Fig. 1. Ternary diagram showing evaporative transformation of silicates composition during light-gas-gun experiments with copper projectile at ~6 km/s. The transformation from starting samples (filled symbols) to condensed material (open symbols) is marked by arrows. Dunite, serpentinite, and harzburgite were used for ultramafic, basalt for mafic, and granite and obsidian for acidic targets. Dashed areas indicate typical composition of terrestrial ultramafic, mafic (basalts), acidic (granites), and alkali (netheline syenites) rocks. From [4].

the main path of evolution of condensed materials by impact simulated vaporization is: ultramafic rocks → mafic rocks → granites → alkali rocks [4] (see Fig. 1).

Formation of the vapor phase proceeds due to re-

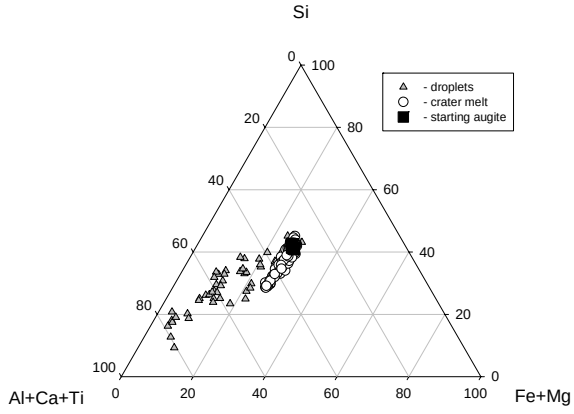

Fig. 2. Ternary diagram showing differentiation trend for melt found on walls of the formed crater and for dispersed melted spherules from starting augite towards Al, Ca, and Ti rich compositions in simulation laser pulse experiment.

lease of volatiles during the boil off of high-temperature impact melt. Depending on the rate of high-temperature processing impact melts have a trend to gain refractory composition [5]. Melts in the beginning of a mass loss process are loosing Si, Fe, alkalis, and their composition enriches in Mg, Ca, Al, and Ti. With a developed mass loss melts loose Mg while Si and even Na are still present in the system. Greater mass loss results in the enrichment of Ca, Al, and Ti in the system (Fig. 2). The end members of the mass loss process depend on the temperature of volatilization. Volatilization under 3000 K results in Al-rich melts and volatilization at temperatures over 3000 K results in Ca-rich melts.

Behavior of trace elements. Experiments also indicate volatile behavior of some typically refractory elements such as U, Th, REE, Zr, and other during impact related heating [6]. Fig. 3 shows the enrichment of formed condensates by REE, Hf, and Zr in laser simulation experiment with basalt. The mechanism of such behavior is not clear. Some experiments (e.g. experiment with anorthosite [7]) show controversial result.

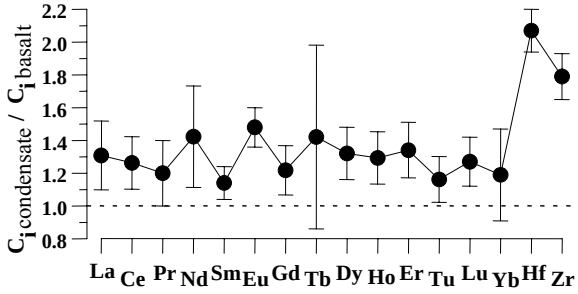

Fig. 3. The ratio of some trace elements concentration in the formed condensate to that in starting basalt after laser pulse simulation experiment. INAA analysis. From [6].

Reduction of iron. An important effect of high-temperature processing is the reduction of iron. Two main mechanisms are responsible for the reduction: thermal and chemical. Thermal mechanism produces metallic iron nano-nucleus through the body of high-temperature siliceous melts due to direct dissociation of iron oxide

$$FeO \rightarrow Fe + O$$

while chemical mechanism involve reducing components (C, H, etc.) in exchange reactions (e.g.)

$$FeO + C \rightarrow Fe + CO$$

Due to immiscibility metallic particles are easily removed from melted silicates. Siderophile elements have a noticeable trend of disproportionation into forming metallic particles and are removed with metallic iron particles into expanding vapor.

Interaction with volatiles. Material of the vapor plume is counteracting with released gases during expansion of the plume. Chemical reactions in hot and dense plume result in formation of volatile rich phases in condensing silicates. Water was trapped by formation of various hydroxides [8]. Carbon was trapped by formation of carbonates, carbides, and organics. Surfaces of forming condensed nanoparticles provide conditions for polymerization of complex hydrocarbons from simple hydrogen- and carbon-containing gases (H_2, H_2O, CO, CO_2, CH_4, etc.) inside an expanding vapor. Experimentally produced hydrocarbons had degree of polymerization up to C_{20} [9]. It is probable that some organics are present in the form of a kerogen-like material. Condensed material is sufficiently richer in volatiles including highly volatile elements compared to depleted impact melt.

Cumulative effect of multiple impacts: Forming condensed material has increased acidity, more rich in volatiles, REE, U, Th, and acquire some other peculiarities, which are typical for crust material. Cumulative amount of vaporized/condensed material was estimated to be ~10% of the total Earth's mass [2] what is more than an order exceeds the mass of present crust. The fate of this condensate is not much understood, whether it was carefully mixed with other materials or could be concentrated in the upper planetary layer to form protocrust. The last possibility can be a result of different properties of impactites. Condensates being more volatile are converted into the vapor plume by secondary impacts more easily and from larger target volume than refractory portion of the mixture. Precipitation of condensates occurs in a thin layer on the planetary surface. This effect may provide preferential transport of condensed materials with growing radius of a planet and their accumulation at surface layer.

The hypothetical impact-induced evaporative differentiation had a competitive effect of early magmatic differentiation resulted from impact-induced heating of planetary interiors. Involvement of volatile rich materials in magmatic processing also provides their preferential melting and floatation to form protocrust. Metallic phases formed in impacts could coagulate and sank in magma to form siderophile rich planetary core.

Acknowledgment: This research was supported by RFBR grant 05-05-64198 and Russian Academy of Sciences program P-18.

References: [1] Benlow A. and Meadows A. J. (1977) *ASS, 46,* 293-300. [2] Gerasimov M. V. and Mukhin L. M. (1979) *Sov. Astron. Lett., 5(4),* 221-223. [3] Gerasimov M. V. (1998) *Earth, Moon, and Planets*, *80(1-3)*, 209-259. [4] Yakovlev O. I. et al. (2000) *Geochem. Intern., 38(10),* 937-954). [5] Gerasimov M. V. et al. (2005) *GSA SP 384*, 351-366. [6] Ivanov L. I. et al. (2001) *Dokl. Akad. Nauk, 377(1),* 30-33 (in Russian). [7] Yakovlev O. I. et al. (2003) *LPSC 34,* #1044. [8] Gerasimov M. V. et al. (2002) *DSR II*, *49(6)*, 995-1009. [9] Gerasimov M. V. and Safonova E. N. (2003) *38th Vernadsky-Brown Microsymposium*, GEOKHI RAS, Moscow, CD-ROM, #MS022.

IMPLICATIONS OF HIT-AND-RUN COLLISIONS BETWEEN DIFFERENTIATED PROTOPLANETS: EVIDENCE FROM IRON METEORITES Joseph I. Goldstein[1], Jijin Yang[1], Edward R. D. Scott[2], G. Jeffrey Taylor[2] and Erik Asphaug[3]. [1]Department of Mechanical and Industrial Engineering, University of Massachusetts, Amherst, MA 01003, USA (jig0@ecs.umass.edu). [2]Hawaii Institute of Geophysics and Planetology, University of Hawaii at Manoa, Honolulu, HI 96822, USA. [3]Center for the Origin, Dynamics and Evolution of Planets, University of California, Santa Cruz, CA 95064, USA.

Introduction: Modeling by Asphaug et al. [1] suggested that colliding Moon-to-Mars sized protoplanets do not simply merge as commonly assumed—in a grazing impact, the smaller planet may escape as a greatly modified body or chain of diverse objects. We present evidence from IVA and other iron meteorites that many irons may come from impactors that experienced such collisions as they had lost most or all of their silicate mantles when they cooled below 1000 K. If the iron meteorites come from bodies that accreted within 1 Myr of CAIs [2] at 1-2 AU as Bottke et al. suggest [3], we infer that protoplanets in the terrestrial planet region were melted by ^{26}Al heating, like the parent bodies of the irons, and that the geological history and chemical composition of the protoplanets may have been modified as a result of hit-and-run collisions that they or precursor bodies experienced when they were partly or largely molten.

Effects of hit-and-run collisions on planetary differentiation and bulk composition: Hit-and-run collisions between protoplanets might drastically disrupt the course of crystallization of their magma oceans (or other substantially melt-rich system). Consider, for example, the Martian magma ocean. Elkins-Tanton et al. [4] constructed geochemically and geophysically reasonable models of the crystallization of the Martian magma ocean, including its overturn caused by an unstable density gradient resulting from initial crystallization. A hit-and-run collision during magma ocean crystallization would scramble any cumulate pile formed up to that time, perhaps resulting in a temporarily stable configuration of the cumulates. Continued crystallization would produce a density gradient atop that rearranged pile. Subsequent overturn would be substantially more complicated than the simpler models predict, perhaps leading to a mantle even more heterogeneous than predicted and a petrologically complex primary crust. In addition, pressure-release melting of either the cumulate pile or originally unmelted regions in the proto-Mars or in the projectile might cause formation of partial melt that can be added to the partially differentiated (and disturbed) magma ocean.

This process could also affect the bulk composition of a protoplanet. There might be loss of the outer portion of a magma ocean or of the initial crust. These areas would consist of differentiated materials, leaving behind a planet depleted and fractionated in incompatible elements, lower in FeO and Fe/Mg, and possibly fractionated in Mg/Si and Al/Si, depending on depth of magma ocean and initial composition. An energetic collision might also deplete a protoplanet in volatile elements. This might not be as severe as for the case of formation of the Moon during a giant accretionary impact, but it could affect the total volatile inventory of the asteroids and terrestrial planets, and perhaps explain the difference in K/Th in the bulk silicate Earth and Mars. H_2O added during accretion could be lost and, thus, need to be added after or during the late stages of accretion.

Evidence for hit-and-run collisions from IVA and other iron meteorites: Most iron meteorites are thought to come from the cores of over 50 asteroids 5-100 km in size, which cooled slowly inside insulating silicate mantles and were then fragmented by impacts [5]. However, this origin is incompatible with the metallographic cooling rates of many irons that vary by factors of 5-100 in each group, as irons from a single well-insulated core should have indistinguishable cooling rates [6, 7]. To help solve this problem, we studied the composition and structure of taenite in group IVA irons, as this group has the largest range of cooling rates [5]. We find that cooling rates for IVA irons at 1000-700 K range from 100 to 6000 K/Myr and increase with decreasing bulk Ni (Fig. 1a). In addition, cooling rates at 600-500 K inferred from the dimensions of the cloudy taenite intergrowths [8] in seven IVA irons vary by a factor of ~10 and are also inversely correlated with bulk Ni (Fig. 1b). These constraints require that the IVA irons crystallized inwards in a 300 km diameter core and were subsequently cooled below 1000 K without any insulating silicate mantle (Fig. 2).

If the core was largely molten at the time of the catastrophic impact, as was inferred to explain the silicates in five IVA irons [9, 10], collisional loss of volatiles may have occurred, as proposed for the Moon and Vesta [11] to account for the extremely low levels of moderately volatile siderophiles in the IVA irons. Ge/Ni values are 0.01-0.001 times chondritic values.

Metallographic cooling rates inferred for groups IIAB, IIIAB, and IVB show ranges of factors of 6-12

(refs. 5-8) suggesting that early partial loss of mantle prior to slow cooling was widespread.

Because catastrophic impacts between asteroid-sized bodies are very inefficient at removing mantle material from cores [13], separation of mantle and core material probably resulted from grazing impacts between Moon-to-Mars sized protoplanets or from tidal stripping of a Vesta-sized or larger body [1].

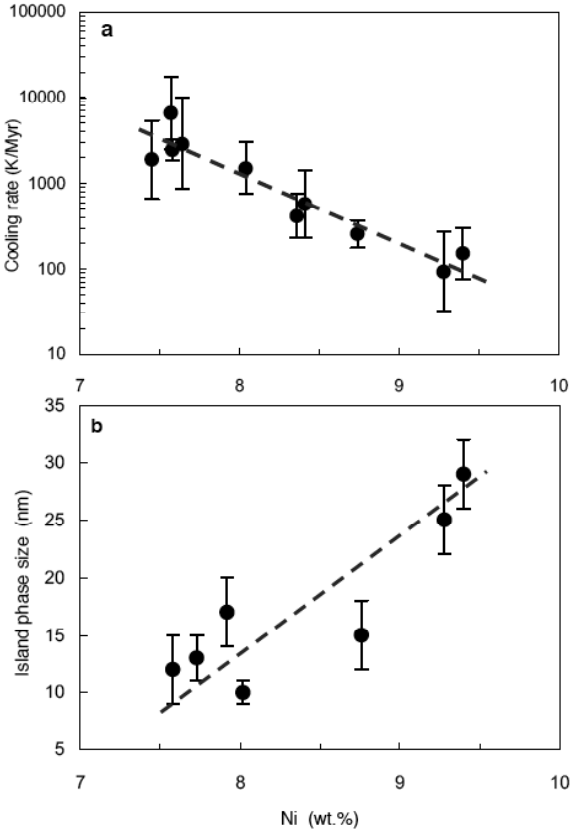

Fig. 1. Estimated cooling rate at 1000-700 K inferred from kamacite growth modelling (a) and the dimensions of the cloudy taenite intergrowth of low-shock irons (b) as a function of bulk Ni concentration for IVA iron meteorites. These data show that the cooling rate of IVA irons decreased with increasing bulk Ni concentration by a factor of ~50 at 1000-700 K, and ~10 at 600-500 K, the temperature range in which cloudy taenite formed.

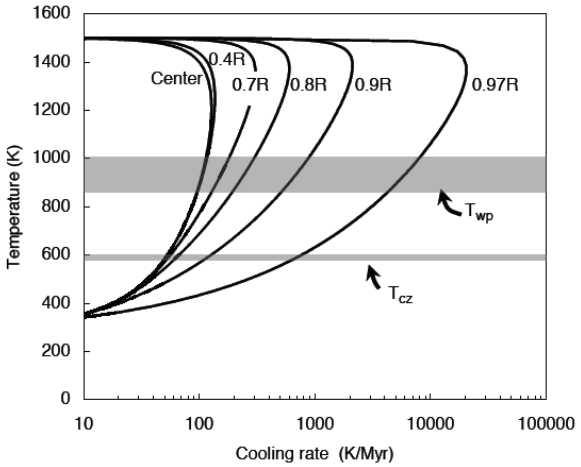

Fig. 2. Cooling rates at different radial locations as a function of temperature for a spherical metallic body exposed to space with a radius R=150 km and an initial temperature of 1500 K. T_{wp} indicates the nucleation temperature for the the Widmanstatten pattern and T_{cz} indicates the start temperature for the cloudy zone microstructure.

References:

[1] Asphaug E. et al. (2006) *Nature*, *439*, 155-160. [2] Kleine T. et al. (2005) *GCA*, *69*, 5805-5818. [3] Bottke W. F. et al. (2006) *Nature*, *439*, 821-824. [4] Elkins-Tanton, L. T., Hess, P. C. and Parmentier, E. M. (2005) *J. Geophys. Res.*, 110, E12S01, doi:10.1029/2005JE002480. [5] Chabot N. L. and Haack H. (2006) In *MESS II* (eds. Lauretta D. S. and McSween H. Y.) 747-771. [6] Haack H. and McCoy T. J. (2003) *Treatise on Geochemistry*, *1*, 325-346. [7] Haack H. et al. (1990) *JGR 95*, 5111-5124. [8] Yang C.-W. et al. (1997) *MAPS*, *32*, 423-429. [9] Haack H. et al. (1996) *GCA*, *60*, 3103-3113. [10] Ruzicka A. and Hutson M. (2006) *MAPS*, in press. [11] Halliday A. N. and Kleine T. (2006) In *MESS II*, 775-801. [12] Burbine T. H. et al. (1996) *MAPS*, *31*, 607-620. [13] Scott E. R. D. et al. (2001) *MAPS 36*, 869-881.

THE HADEAN EARTH T. M. Harrison (Institute of Geophysics and Planetary Physcis & Dept. of Earth and Space Sciences, UCLA, Los Angeles, CA 90095, U.S.A.) and Project MtREE.

Introduction: The Hadean Eon (4.5-4.0 Ga) is the dark age of Earth history; there is no known rock record from this period. However, detrital zircons as old as nearly 4.4 Ga from the Jack Hills, Western Australia, offer unprecedented insights into this formative phase of Earth history. Investigations using these ancient zircons suggest that they formed by a variety of processes involving a hydrosphere within ~200 m.y. of planetary accretion and challenge the view that continental and hydrosphere formation were frustrated by meteorite bombardment and basaltic igneous activity until ~4 Ga.

The Mission to Really Early Earth (MtREE): MtREE is an international consortium using Hadean zircons to investigate the earliest evolution of the atmosphere, hydrosphere, and continental lithosphere. However, these experiments require large quantities of >4 Ga zircons which are both small (typically 1-5 μg) and rare (~3%) in the detrital zircon population. To this end we have dated over 80,000 Jack Hills zircons to identify some 2500 Hadean grains which are being used in a variety of studies including: stable isotope analyses, single crystal Xe isotopic analyses to document the terrestrial Pu/U ratio, and initial $^{176}Hf/^{177}Hf$ and $^{142}Nd/^{144}Nd$ studies. The inclusion mineralogy of these ancient zircons points towards their origin in diverse but seemingly familiar petrogenetic settings. Xe isotopic results indicate that mantle-derived Xe isotopes cannot be interpreted in terms of the age of the atmosphere in a straightforward manner, but Hf isotopes indicate the existence of terrestrial continental crust as early as 4.5 Ga and that a mature sedimentary cycling system operating throughout the Hadean. In general, these first direct observations of the Hadean Earth appear to contradict most of our familiar assumptions about this period.

Origin of the hydrosphere: The observation of a heavy oxygen isotope signature in some Hadean zircons led Mojzsis et al. [1] to propose that the protolith of these grains contains ^{18}O-enriched clay minerals which in turn implies that liquid water was present at or near the Earth's surface by ca. 4.3 Ga. The presence of hydrated mineral inclusions of peraluminous character was taken as further evidence of a Hadean hydrosphere [1]. Using a new crystallization thermometer, Watson and Harrison [2], found that Hadean zircon crystallization temperatures cluster strongly at 680±25°C, similar to that of granitoid zircon growth today, substantiating the existence of wet melting conditions throughout the Hadean. This peak further suggests that an excess of water was available during prograde melting relatively close to the Earth's surface.

Origin of the continental crust: The long favored paradigm for continent formation is that initial growth was forestalled until ~4 Ga and then grew slowly until present day. However, a minority view [3] has persisted that continental crust was widespread during the Hadean. Initial $^{176}Hf/^{177}Hf$ ratios of Jack Hills zircons ranging in age from 3.96 to 4.35 Ga show surprisingly large positive and negative isotope heterogeneities indicating that a major differentiation of the silicate Earth occurred at ~4.5 Ga [4]. A likely consequence of this differentiation is the formation of continental crust with a volume of similar order to the present, possibly via the mechanism described by Morse [5].

Hadean plate boundary interactions?: The inclusion mineralogy of these ancient zircons include meta- and peraluminous assemblages suggestive of two forms of convergent margin magmatism. We interpret the 680±25°C zircon crystallization peak as due to minimum-melting during prograde heating, consistent with thrust burial. These data, and the seeming disappearance of the strongly positive and negative $^{176}Hf/^{177}Hf$ ratios by the early Archean, suggest that the Earth had settled into a pattern of crust formation, erosion, and sediment recycling by ~4.3 Ga similar in many respects to the known era of plate tectonics. New ideas regarding the feasibility of plate boundary interactions during the Hadean and independent evidence of widespread mantle depletion within 50 m.y. of Earth formation attract comparisons between >4 Ga plate interactions and the contemporary plate tectonic system. Our data tends to support the view of Armstrong [3] that the Earth almost immediately differentiated into relatively constant volume core, depleted mantle, enriched crust, and fluid reservoirs. Our results support the view that continental crust was a component of the enriched counterpart that formed at 4.5 Ga, but that this original crust had largely been recycled back into the mantle by the onset of the Archean.

References: [1] Mojzsis S.J., Harrison, T.M. and Pidgeon R.T. (2001) *Nature, 409*, 178. [2] Watson E.B. and Harrison T.M. (2005) *Science, 308*, 841. [3] Armstrong R.L. (1981) *Phil. Trans. Roy. Soc. Lond. Series, A* 301, 443. [4] Harrison T.M. et al. (2005) *Science, 310*, 1947. [5] Morse S.A. (1987) *EPSL, 81*, 188.

METAL-SILICATE SEGREGATION IN ASTEROIDAL METEORITES. J. S. Herrin and D. W. Mittlefehldt, NASA/Johnson Space Center , Houston, TX, USA (jason.s.herrin1@jsc.nasa.gov).

Introduction: A fundamental process of planetary differentiation is the segregation of metal-sulfide and silicate phases, leading eventually to the formation of a metallic core. Asteroidal meteorites provide a glimpse of this process frozen in time from the early solar system. While chondrites represent starting materials, iron meteorites provide an end product where metal has been completely concentrated in a region of the parent asteroid. A complimentary end product is seen in metal-poor achondrites that have undergone significant igneous processing, such as angrites, HED's and the majority of aubrites. Metal-rich achondrites such as acapulcoite/lodranites, winonaites, ureilites, and metal-rich aubrites may represent intermediate stages in the metal segregation process. Among these, acapulcoite-lodranites and ureilites are examples of primary metal-bearing mantle restites, and therefore provide an opportunity to observe the metal segregation process that was captured in progress. In this study we use bulk trace element compositions of acapulcoites-lodranites and ureilites for this purpose.

Discussion: For a given starting mass, metal-silicate segregation occurs in three stages each brought about by an increase in temperature: (1) textural coarsening of silicate and metal grains, (2) formation and migration of metal-sulfide partial melts, and (3) migration of refractory metal *en masse*. Silicate melting and melt migration accompanies, and may facilitate, this stage. The first stage can be observed in the metamorphic stages (3-6) of ordinary chondrites which experienced an increase in mean grain size and mineral equilibrium with progressive metamorphism at subsolidus temperatures.During this stage, siderophile elements remain unfractionated in the bulk mass. The second stage begins as temperatures exceed the Fe-Ni-S cotectic (~980ºC). Sulfur-

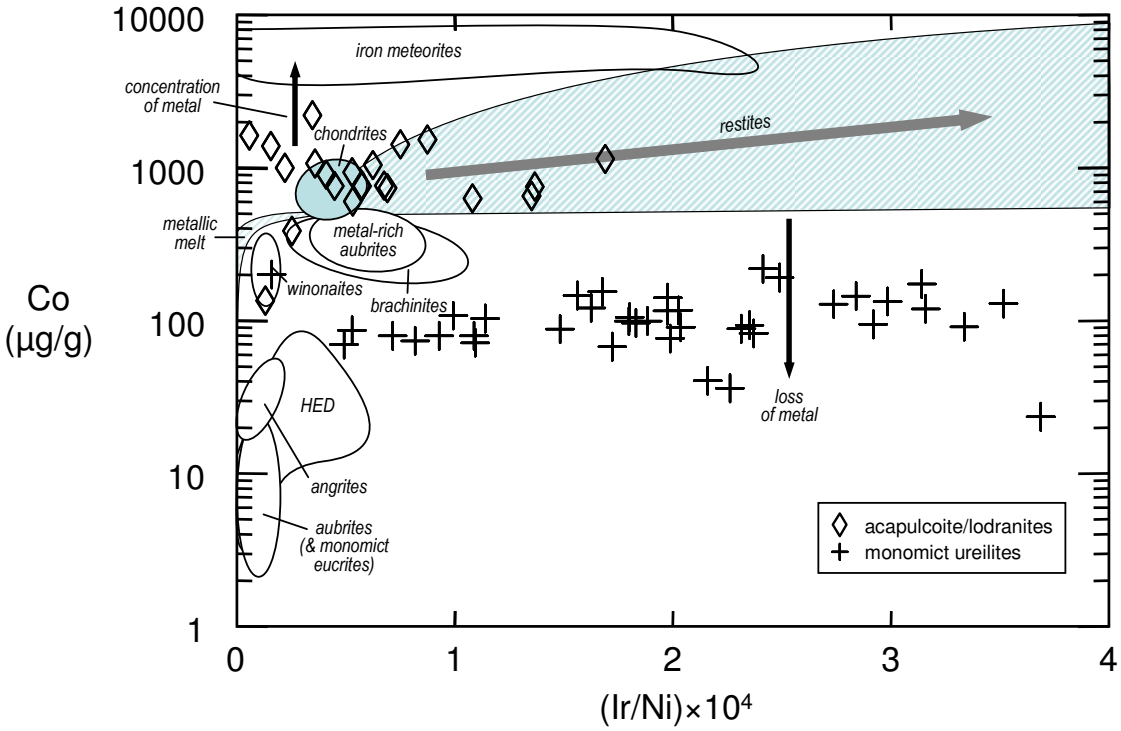

Figure 1. Siderophile elements Ir/Ni (by weight) vs. Co for asteroidal meteorites. Ir/Ni increases through extraction of metallic partial melts while Co concentration is an indication of metal abundance. Field labeled "chondrites" encompasses all known chondrite types. Field for restite composition is based on batch melt extraction from a CI chondrite parent material at melt S contents of 0-44 mol% and with 0-20% coeval loss of surrounding silicate. A field for complimentary aggregate melts (in a constant relative volume of silicate) is also shown. Assuming a chondritic precursor material, compositions below these fields require additional loss of metal while those above require concentration of metal. Acapulcoite/lodranite and ureilite compositions are indicated by symbols. Generalized data fields are drawn for other meteorite types to encompass >90% of available data. Metal-rich aubrites are distinguished by a separate field from other aubrites. The lower aubrite field overlays and is nearly identical to that of monomict eucrites. The HED field is taken to represent the vast majority of uncontaminated group members. Diogenites occupy the portion of the field in view while monomict eucrites are overlain by the lower aubrite field and encompass nearly the same portion of the diagram. A few cumulate eucrites plot slightly to the right of the field. Data compiled from numerous sources.

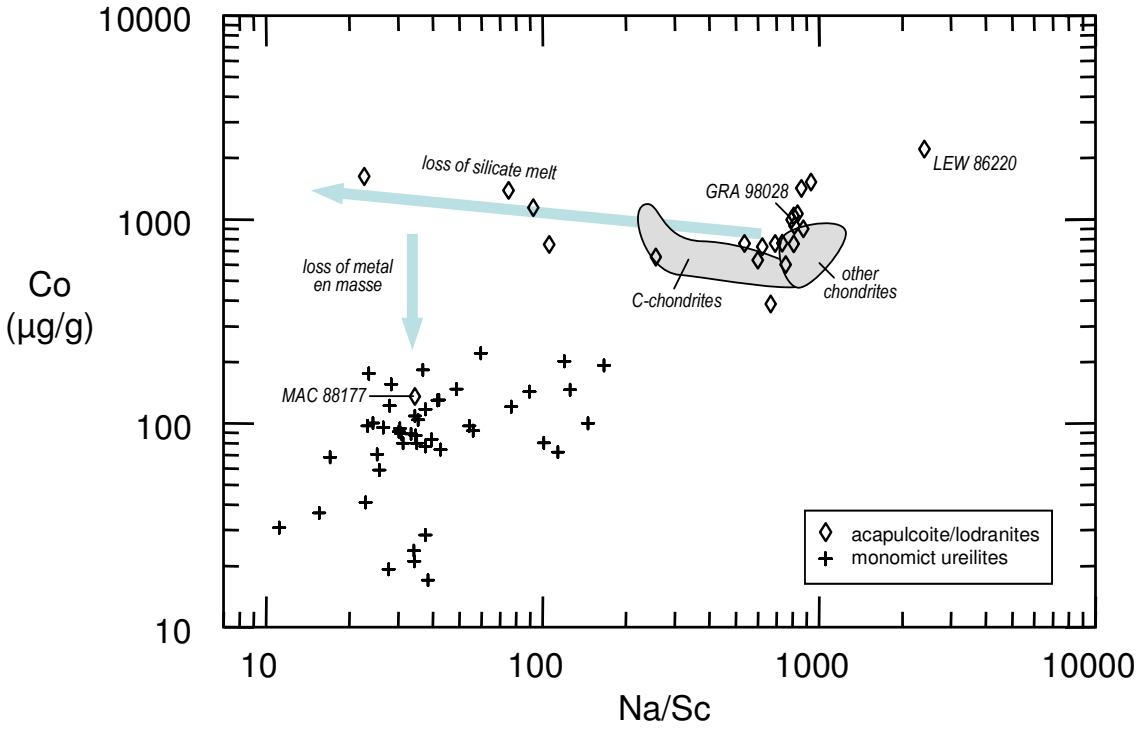

Figure 2. Processes of silicate partial melt extraction, indicated by decreasing Na/Sc, and extent of metal loss, indicated by Co concentration, for acapulcoite-lodranites and monomict ureilites. GRA 98028 is the most texturally primitive acapulcoite [1] and represents a logical starting composition on the figure. MAC 88177 is a lodranite which has lost much or all of its original metal. LEW 86220 is an acapulcoite enriched with a basaltic melt [2,1]. Data compiled from numerous sources.

rich partial melts form and can continue to form until S is exhausted from the system. Combined textural and chemical evidence suggest that these melts readily migrate into and out of portions of the parent asteroid even in the absence of silicate melt migration and even at temperatures below the silicate solidus [2,3]. At this stage, siderophile elements become fractionated according to their solid-liquid partitioning behavior. Figure 1 shows elevated Ir/Ni in acapulcoite-lodranites and ureilites consistent with removal of S-rich metallic partial melts, which would have very low Ir/Ni. All other groups of stony asteroidal achondrites are characterized by near-chondritic or sub-chondritic Ir/Ni. Stage 3 is the near complete removal of metal from silicate. If S is effectively exhausted during stage 2, the remaining solid metal is extremely refractory, and will not melt until temperatures well above the silicate solidus. Complete loss of this remaining Fe,Ni-metal alloy by strictly mechanical means would require high degrees of silicate partial melting, deformation, or both [4]. Low siderophile element concentrations in monomict ureilites, represented by Co in Figure 1, suggest that much of their refractory metal component has indeed been lost. Ureilites are estimated to have experienced ~30% depletion of silicate partial melts to account for their chemical and mineralogic composition [5,6]. All acapulcoite-lodranites with the exception of MAC 88177 appear to retain a significant metal component. MAC 88177 is also unique in that it appears to have experienced a greater extent of silicate partial melt extraction than other clan members, estimated to exceed 10% [2,1]. Figure 2 shows that significant silicate melt loss appears to be a prerequisite for the removal of metal. The underlying cause for greater efficiency of metal segregation in ureilites could be the greater size of the ureilite parent body, which is constrained to diameters of >100 km by the pressure-dependent retention of C [6]. Estimates of the size of the acapulcoite-lodranite parent body, meanwhile, are in the 10's of km [2]. Greater parent body size has a two-fold effect. The first being greater thermal insulation, allowing internal portions of the body to retain radiogenic heat and reach higher temperatures (ureilites yield olivine-pigeonite temperatures of 1150-1300ºC [7] while acapulcoites commonly yield 2-pyroxene temperatures in the range 1000-1150ºC [8]). The second effect being increased force of gravity at a given depth below the asteroidal surface, which would enhance buoyancy driven segregation of dense metallic melts.

Conclusions: The acapulcoite-lodranite clan and ureilites are unique in that they preserve a depleted asteroidal mantle sequence that retains refractory primary metal in silicate matrix. In acapulcoite-lodranites, metal segregation is largely limited to extraction of metallic partial melts (stage 2), while ureilites appear to have experienced the removal of some of their refractory metal component (stage 3). This difference could be rooted in the larger size of the ureilite parent body. In the future, as more meteorites are recovered and more data is obtained on existing meteorites, other more underrepresented groups of stony asteroidal achondrites might yield similar sequences of refractory metals.

References: [1] Patzer A *et al.* (2004) *M&PS*, 39(1):61-85. [2] McCoy TJ *et al.* (1997) *GCA*, 61(3):639-650. [3] Mittlefehldt DW *et al.* (1998) *Rev Min*, 36:(4)1-195. [4] Rushmer T *et al.* (2005) *EPSL*, 239(3-4):185-202. [5] Goodrich CA (1992) *Meteoritics*, 27:327-252. [6] Goodrich CA (2002) LPSC 33 #1379. [7] Singletary SJ & Grove TL (2003) *M&PS*, 38(1):95-108. [8] McCoy TJ *et al.* (1997) *GCA*, 61(3):623-637.

THE INITIAL STATES OF THE TERRESTRIAL PLANETS EMBEDDED IN THE SOLAR NEBULA. M. Ikoma[1] and H. Genda[2], [1]Research Center for Evolving Earth and Planets, Tokyo Institute of Technology, 2-12-1 I2-26, Ookayama, Meguro-ku, Tokyo, Japan, 152-8551: mikoma@geo.titech.ac.jp, [2]Department of Earth and Planetary Sciences, Tokyo Institute of Technology, 2-12-1 Ookayama, Meguro-ku, Tokyo, Japan, 152-8551: genda@geo.titech.ac.jp

Introduction: The accretion process in the final stages of terrestrial planet formation in the solar system is a matter of controversy. A key issue is what damped eccentricities of the planets. Planetary embryos grow in an oligarchic fashion; a planetary embryo outgrows surrounding planetesimals, but grows more slowly than smaller embryos in other regions [1]. In the final stages, there occur several giant collisions between those oligarchic bodies to form full-sized planets. Planets formed in this way have high eccentricities [2], which must be damped to the current low eccentricities of the terrestrial planets. One possibility is the drag of nebula gas [3, 4]; the other possibility is dynamical friction of remaining planetesimals [5, 6]. Each scenario would yield different initial states of the planets.

In this paper we focus on the former possibility. We simulate the atmospheric structure of a planet embedded in the solar nebula, calculate the surface temperature and pressure, and then discuss the thermal state of the mantle and the origin of water of the Earth.

Surface temperature and pressure: We simulate the spherically-symmetric hydrostatic structure of the atmosphere that connects with the surrounding nebula. We assume the nebular temperature is 280K, while we regard the nebular density (ρ_n) as a parameter to take into account a possibility of terrestrial planet formation in a dissipating nebula. The atmospheric composition is assumed to be solar. The equation of state of the atmospheric gas is the nonideal one [7]. The gas opacity is taken from [8]. The grain opacity is assumed to be 0.01 times that given by [9].

The top and bottom panels of Figure 1 show the surface temperature and pressure, respectively, as a function of heat flux for Earth-mass (*solid line*) and 0.1-Earth-mass (*dashed line*) planets for nebular density equal to that of the minimum-mass solar nebula (ρ_{MSN} = 1.2x10^{-9} g/cm^3) [10]. In accretion stages, the heat flux is supplied mainly by planetesimals. As the number of remaining planetesimals decreases, the heat flux decreases with time. For example, if the accretion rate of planetesimals is 1x10^{-8} M_E/yr (M_E: Earth mass), the heat flux (L) is 1x10^{24} erg/sec for a 1M_E planet and L = 1x10^{23} erg/sec for a 0.1M_E planet (hereafter a Mars-mass planet). However, the actual values are still uncertain.

The surface temperature of an Earth-mass planet is rather insensitive to the heat flux and is always higher than 2000K (the top panel of Figure 1). Unlike Earth-mass planets, the surface temperature of a Mars-mass planet decreases rapidly as the heat flux decreases.

The surface pressure of an Earth-mass planet increases as the heat flux decreases (the bottom panel of Figure 1). The surface pressure is as high as more than 10^8 Pa for L < 1x10^{24} erg/sec. For a Mars-mass planet,

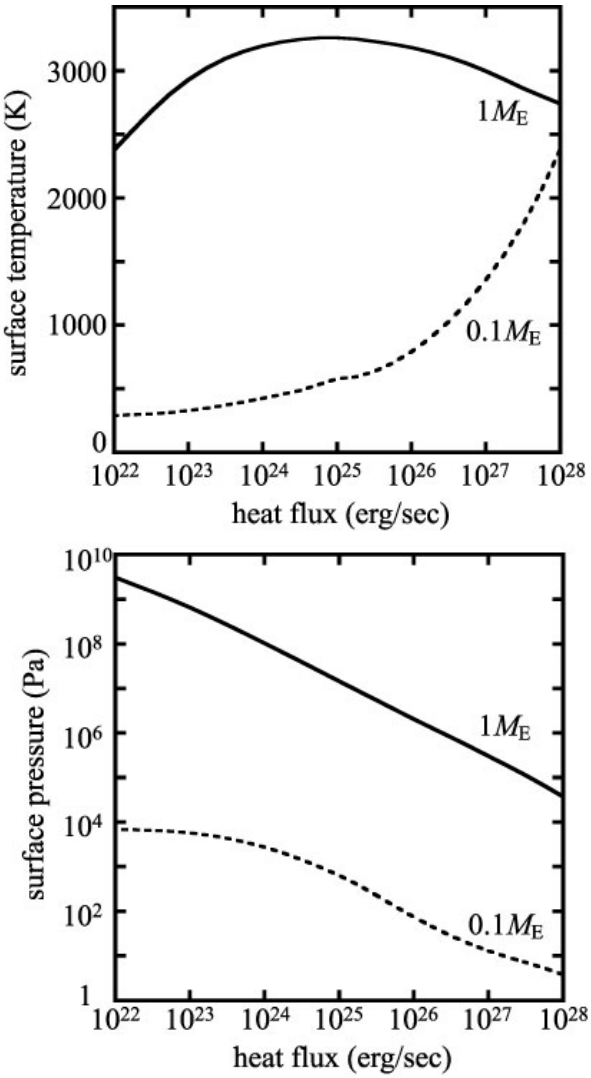

Fig. 1.—Surface temperature (*top*) and surface pressure (*bottom*) of a 1 M_E planet (*solid line*) and 0.1 M_E planet (*dashed line*) as a function of heat flux for nebular density equal to that of the minimum-mass solar nebula.

the surface pressure increases as the heat flux decreases, but flattens off at $L \sim 1\text{x}10^{24}$ erg/sec.

Figure 2 shows the surface temperature of an Earth-mass planet as a function of the nebular density normalized by ρ_{MSN}. The surface temperature decreases as the nebular density decreases. However, the dependence is quite small. Even for $\rho_n = 1\text{x}10^{-10}\rho_{MSN}$, the surface temperature is higher than 1500K (~ melting temperature of silicate mantle). The surface pressure is rather insensitive to the nebular density as well; the surface pressure decreases only by 1-2 orders of magnitude, even if the nebular density decreases to $1\text{x}10^{-10}\rho_{MSN}$ [11].

Production of Water: An Earth-mass planet embedded in the solar nebula gets a large amount of hydrogen. Since the surface temperature is almost always higher than 1500K, the molten surface is kept for a long time. In that case water can be produced through the reaction between the atmospheric hydrogen and oxides (i.e., FeO) contained in the planet [11]. In chemical equilibrium, water vapor comparable in mass with hydrogen is produced [12]. As implied by Figure 1, this mechanism of water production does not work on a Mars-mass planet except for cases of extremely high heat flux.

If the water vapor condenses to form an ocean, the mass of the ocean is comparable with or larger than the current mass of the Earth's ocean. The water vapor has the deuterium/hydrogen (D/H) ratio higher by a factor of 5-7 than that of the current Earth's ocean. However, deuterium exchange between the ocean and the hydrogen-rich atmosphere at low temperatures and subsequent mass fractionation during the hydrodynamic escape of the hydrogen are able to make the ocean so rich in deuterium that the D/H of the ocean is consistent with the current value [13].

Magma Ocean of the Early Earth: The surface temperature of an Earth-mass planet has been found to be higher than 1500K for wide ranges of heat flux and nebular density. This means that a magma ocean continues to exist until the solar nebula dissipates almost completely ($\rho_n < 10^{-10}\ \rho_{MSN}$). Although the lifetime of the nebula is often considered to be $< 1\text{x}10^7$ yr [14], the lifetime of the magma ocean might be much longer because such low nebular densities are beyond the detection limit.

The magma ocean is likely to be rather deep. If we include the effect of water vapor in our simulations, the surface temperatures are higher than those obtained here because of its blanketing effect and large molecular weight. Furthermore the water dissolves into the magma ocean. The melting temperature of a wet silicate is known to be significantly lower than that of a dry silicate [15].

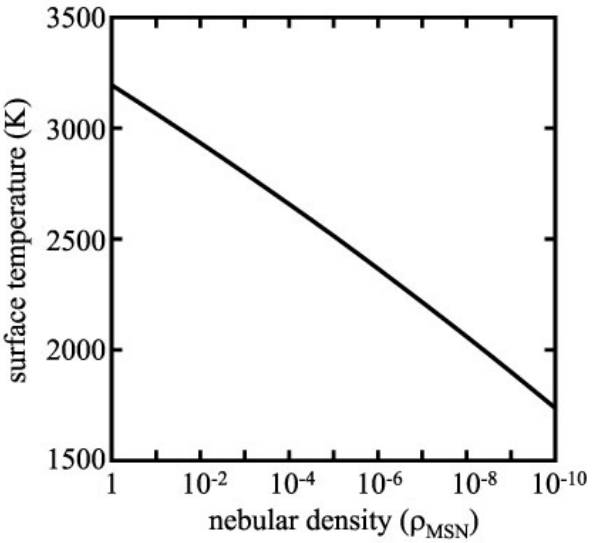

Fig. 2.—Surface temperature of a $1M_E$ planet as a function of the nebular density normalized by that of the minimum-mass solar nebula (ρ_{MSN}) for $L = 1\text{x}10^{24}$ erg/sec.

Conclusions: If the terrestrial planets had formed in the solar nebula, as suggested by several theories of the terrestrial planet formation, the Earth would have had a massive hydrogen-rich atmosphere; its blanketing effect is great enough to keep the surface molten for a long time. The reaction between the atmospheric hydrogen and oxides of the mantle produced a comparable amount of water with the current ocean. Since the water vapor increases the surface temperature and the water dissolved in the magma ocean decreases the melting temperature of silicate, there existed a quite deep magma ocean. The situation would be similar on Venus [11], but quite different on Mars.

References: [1] Kokubo E. and Ida S. (2006) *Icarus*, 143, 171. [2] Chambers J. E. et al. (1996) *Icarus* 119, 261. [3] Kominami J. and Ida S. 2002 *Icarus*, 157, 43. [4] Nagasawa M. et al. (2005) *ApJ* 635, 578. [5] Raymond S. N. et al. (2006) *Icarus* 183, 265. [6] O'brien D. P. et al. (2006) *Icarus* 184, 39. [7] Saumon D et al. (1995) *ApJS* 99, 713. [8] Alexander D. R. and Ferguson J. W. (1994) *ApJ* 437, 879. [9] Pollack J. B. et al. (1985) *Icarus* 64, 471. [10] Hayashi C. (1981) *Prog. Theor. Phys. Suppl.* 70, 35. [11] Ikoma M. and Genda H. (2006) *ApJ* 648, 696. [12] Robie R. A. et al. (1978) *US. Geol. Surv. Bull.*, 1452. [13] Genda H. and Ikoma M. (2006) *Icarus,* submitted. [14] Natta A. et al. (2000) *in Protostars and Planets IV*, ed. V. Mannings et al. (Tucson: Univ. Arizona Press), 559. [15] Zahnle K. J. et al. (1988) *Icarus* 74, 62.

ISOTOPIC CONSTRAINTS ON THE TIMESCALES OF EARTH'S DIFFERENTIATION. S. B. Jacobsen[1], M. C. Ranen[1] and M. I. Petaev[1,2], [1]Dept. of Earth and Planet. Sci., Harvard Univ., 20 Oxford St., Cambridge, MA 02138 (jacobsen@neodymium.harvard.edu) [2]Harvard-Smithsonian CfA, 60 Garden St., Cambridge, MA 02138.

Introduction: Long-lived chronometers (Rb-Sr, Sm-Nd, Lu-Hf and U-Th-Pb) point to a prolonged differentiation of the Earth's crust and mantle with a mean crustal extraction age of ~ 1.8 Ga [1]. The very small volume of early (>3.5 Ga) Archaean crust preserved today (less than 1% of the present continental volume) has been interpreted as indicating that crustal growth did not begin until about 4.0 Gyr ago, before which the silicate Earth remained well mixed and essentially undifferentiated. However, the inferred initial $^{143}Nd/^{144}Nd$ ratios of many early Archean rocks are higher than that of the bulk Earth implying that by 3.8 Ga ago the volume of the crust must have been as large as about 40% of the present value [2]. Studies of Nd and Hf isotopic variations in the oldest terrestrial samples point to a significant early silicate differentiation within the first 100 Myr of Earth's formation [2,3]. Better constraints of the earliest history can be placed by the now extinct nuclides ^{146}Sm and ^{182}Hf [4,5].

The Isotopic Evolution of the Bulk Earth: The Early Solar System (ESS) may not have been as well mixed with respect to heavy isotopes as previously thought. The nucleosynthetic processes which produced all the heavy elements (r-,s-,p-processes, neutron burst) did not necessarily homogenize themselves to the extent that various planetary bodies have the same initial isotopic composition of the heavy elements [6]. This has been shown for Mo, Zr, Os and Nd, with the bulk chondrites being enriched in the r-process or the neutron burst process compared to the s-process. To further investigate the effects of incomplete nebular mixing we [7] have studied the Ba isotopic composition of carbonaceous and ordinary chondrites. All samples studied show an excess of up to 50 ppm in the $^{138}Ba/^{136}Ba$ ratio compared to the Earth when normalized to $^{134}Ba/^{136}Ba$, two s-only nuclides. This is consistent with an r-process excess (^{138}Ba is made by both the r- and the s-processes) or a neutron burst component excess (Fig. 1).

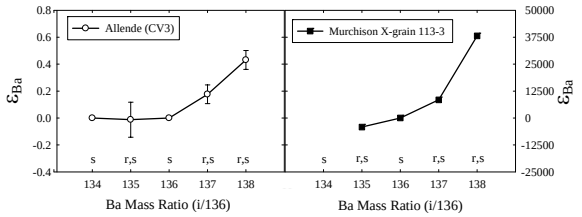

Figure 1. Ba isotope heterogeneities [7].

The only way that Ba isotope differences can exist between bulk planetary bodies is by incomplete mixing of nucleosyntheic components, not by fractionation within a planet. The Ba data predict a deficit in ^{142}Nd (an s-only nuclide) in chondrites suggesting that the $^{142}Nd/^{144}Nd$ differences between chondrites and the Earth are not due to Sm/Nd fractionation and/or ^{146}Sm decay in the early Earth, but rather that the ESS was not perfectly mixed with regard to the carrier grains of different nucleosynthetic processes (Fig. 2).

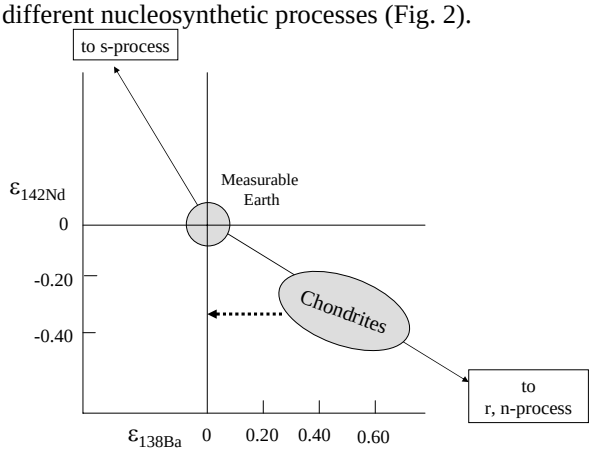

Figure 2. Cartoon of Ba and Nd isotopic variations in Solar System materials.

We need a better understanding of how to use the isotope heterogenities in chondrites to infer the correct initial isotopic compositions for various Solar System objects, such that sufficiently accurate bulk evolutions of ratios like $^{142}Nd/^{144}Nd$ can be estimated. This will involve both clearly identifying the mixture of nucleosynthetic components and understanding how the observed range of values are set in the solar system through evaporation and condensation processes of grains containing the most refractory elements.

The Timescale of Core Formation: The isotopic constraints on the time scales of formation of metal cores in the terrestrial planets will be reviewed. Both Earth and Mars exhibit radiogenic W-isotopic compositions compared to the average Solar System composition, demonstrating that they formed while ^{182}Hf (half-life 9 Myr) was extant in Earth and decaying to ^{182}W. Based on the ^{182}Hf-^{182}W chronology, the mean times of core formation in Earth and Mars are ~10 and ~3 Myr after Solar System formation, with the total times being about 30 and 10 Myr, respectively [5]. Core formation in the asteroid Vesta is constrained to be even earlier with a mean time of ~ 0.8 Myr. This

implies that the terrestrial planets underwent early and rapid accretion and core formation that ended by ~ 30 Myr after the origin of the Solar System. Various authors have argued that the U-Pb system requires a longer timescale (cf. [8]), but this is only one of many possible interpretations of the U-Pb isotopic system. Part of the problem lies in the different behavior and interpretation of long-lived versus extinct isotope systems [4].

The Timescale of Early Crust Formation: Consideration of ^{147}Sm-^{143}Nd systematics and the apparently low rate of coninent recycling before 4 Ga ago, suggests that primordial differentiation of the Earth may have begun ~4.5 Ga ago. Strong evidence for such early differentiation comes from measurements of ^{143}Nd/^{144}Nd and ^{142}Nd/^{144}Nd ratios in a ~3.8-Ga-old supracrustal rock from Isua, West Greenland [9,4]. Coupled ^{146,147}Sm-^{142,143}Nd systematics suggest that fractionation of Sm/Nd took place ~4.47 Ga ago, due to extraction of a light-rare-earth-element-enriched primordial crust. Differences in the ^{142}Nd/^{144}Nd ratio between Earth and chondrites have been attributed to the formation of an early enriched crust that subsequently sunk to the core-mantle boundary, cut off from other mantle processes [10]. However, this scenario is called into question with the results of the Ba data showing that the Earth is expected to have a different ^{142}Nd/^{144}Nd composition caused by incomplete mixing of the solar nebula so that no recycled crust would be cut off from the bulk silicate mantle.

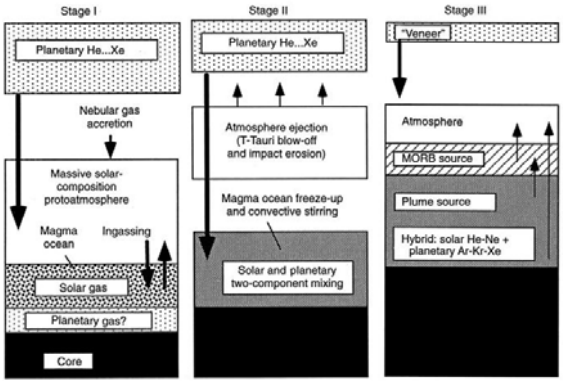

Figure 3. Early atmosphere evolution from [11].

Early Atmospheres and Late Veneers: Based on noble gas evidence a schematic three-stage evolution of Earth's core-mantle-atmosphere system during accretion has been proposed [11]. Stage I is initiated when the proto-Earth grows large enough to accrete a massive H_2-He protoatmosphere directly from the nebular gas. Under these conditions, the blanketing effect of the massive protoatmosphere supports a global magma ocean into which solar gases dissolve and through which metal rains out to form the proto-core. This scenario was suggested to explain the origin of the solar component in the deep Earth. Continued accretion of planetesimals (containing planetary noble gases) occurs during all stages, but their contribution is totally overwhelmed by the existing protoatmosphere interacting with the magma ocean during stage I. Stage II begins when the massive protoatmosphere was blown off by intense proto-solar radiation, causing the magma ocean to freeze due to a rapid heat loss in a "naked" (no atmosphere) phase. The final, present stage III began when the solar ultraviolet luminosity decreased to a level allowing an atmosphere to be retained and grown by mantle degassing and accretion of volatile-rich objects ("late veneer") scattered from the outer nebula (C1 meteorites and comets).

Comparison with other Solar System Bodies: There is now a substantial body of radiogenic isotopic data (Sr, Nd, Hf, Pb, Os, W, Zr) that provides important clues to the evolution of martian mantle and crustal reservoirs over the entire course of its long geologic history. Many of these studies have emphasized a wide-spread early global differentiation at about 4.5 Ga, with very little happening later. The SNCs are samples of martian crust that were extracted at various times from the martian mantle and thus offer a view of the martian isotopic evolution. The sample ALH 84001 indicates that a mafic-ultramafic crust was extracted from the martian mantle as early as 4.5 Ga. Aslo, isotopic studies of SNCs indicate that the mantle was already depleted at ~4.5 Gyr; ε_{Nd} evolved to 15 by 1.3 Ga, and was in the range 20 - 50 at 0.2 Ga. The Nd and Sr isotope data constrain the mean age of formation of the martian crust to ~3.6 ±0.6 Ga. Also, any significant crustal recycling can only have happened in the very earliest history of Mars. Based on all available isotopic and trace element data for martian meteorites we obtain a mean age of formation of the crust on Mars of ~ 3.4 ±0.6 Ga, with about half of this crust being formed at 4.5 Ga. This demonstrates substantial and prolonged crustal formation on Mars subsequent to 4.5 Ga.

References: [1] Jacobsen S. B and Wasserburg G. J. (1979) *JGR, 84,7411-7427.* [2] Jacobsen S. B. and Dymek R. F. (1988) *JGR, 93,* 338-354. [3] Bizzarro M. et al. (*2003) Nature*, 421, 931-933. [4] Jacobsen S. B. and Harper C. L. (1996) *Geophysical Monograph* 95, Am. Geophys. Union, 47-74. [5] Jacobsen S. B. (2005) *Annu. Rev. Earth Planet. Sci*. 33, 531-570. [6] Harper and Jacobsen (1993) *LPSC*, 24, 607-608. [7] Ranen and Jacobsen (2006) *Science*, in review. [8] Halliday A. N. (2004) *Nature* 427, 505–509. [9] Harper and Jacobsen (1992) *Nature*, 360, 728-732. [10] Boyet and Carlson (2005) *Science*, 309, 576-581. [11] Harper and Jacobsen (1996) *Science*, 273, 1814-1818.

EARLY PLANETARY DIFFERENTIATION: COMPARATIVE PLANETOLOGY. J.H. Jones, KR, NASA/JSC, Houston, TX 77058 (john.h.jones@nasa.gov).

Introduction: We currently have extensive data for four different terrestrial bodies of the inner solar system: Earth, the Moon, Mars, and the Eucrite Parent Body [EPB]. All formed early cores; but all(?) have mantles with elevated concentrations of highly siderophile elements, suggestive of the addition of a late "veneer". Two appear to have undergone extensive differentiation consistent with a global magma ocean. One appears to be inconsistent with a simple model of "low-pressure" chondritic differentiation. Thus, there seems to be no single, simple paradigm for understanding early differentiation.

EPB. Currently, there is no evidence that eucrites are other than simple partial melts of a chondritic (CO-like) parent body. The agreement between phase equilibrium experiments on natural eucrites and devolatilized Murchison (CM) is remarkable. The most compelling reason for believing that eucrites might be the result of equilibrium or fractional crystallization of a more primitive magma is the desire to relate eucrites and diogenites (i.e., howardites). But at this juncture, no model has been able to produce such a relationship in a quantitatively satisfying way. Both partial melting experiments of chondrites and constraints from eucrite Sc/La ratios imply that eucrites were produced by ~20% partial melting of a CO-like source. Such a source is depleted in low-Ca pyroxene by 1200°C, with a maximum MgO content of ~En_{70}, whereas almost all diogenites have Mg#'s > 70. Experiments show that eucrites formed at IW-1, consistent with a chondritic ol-opx-metal assemblage.

The EPB differentiated very early while ^{182}Hf was still present ($t_{1/2}$ = 9 m.y.). Therefore, eucrite petrogenesis occurred much less than 50 m.y. after CAI formation. Since the EPB appears to have experienced core formation, this means that core formation occurred at this time, or earlier.

Lithophile incompatible elements were quantitatively removed from the eucrite source regions. Incompatible element ratios in eucrites are generally chondritic.

The Moon. The Moon is the type locality for the magma ocean hypothesis. Mare basalts (and their source regions) are depleted in alumina and have negative Eu anomalies. Conversely, the highlands crust is enriched in plagioclase and has a positive Eu anomaly. Therefore, there is a natural complementarity between these two reservoirs, suggesting separation of a plagioclase component by floatation from a magma ocean.

Even if this separation occurred without the aid of a magma ocean, the chemical complementarity between the lunar highlands and the depleted mare source regions is undeniable. Melt was clearly extracted from the lunar interior early in its history, depleting the lunar mantle in incompatible elements. These incompatibles were concentrated into a reservoir known as KREEP. The uniformity of elemental ratios in KREEP is itself an argument for a magma ocean — i.e., a single event.

Model ages of KREEP are nearly concordant between several different chronometer systems: 4.35-4.45. This suggests that the magma ocean lasted about 200 m.y. Perhaps coincidentally, this is the age of lunar differentiation inferred from ^{142}Nd systematics. Therefore, there are hints that early lunar differentiation lasted for quite some time.

Unlike the EPB, ^{182}W anomalies in lunar samples are small to nonexistent. This suggests that, even though lunar differentiation was prolonged, it was not initiated until ^{182}Hf was nearly extinct. These observations would also be consistent witth a Moon that differentiated quickly at ~4.35 b.y. and that inherited a small ^{182}W anomaly.

It is now generally believed that the Moon has a small core, consistent with the redox conditions inferred earlier.

Experiments show that lunar basalts formed near IW-1, similar to eucrites.

Unlike the EPB(?), there are enclaves of the lunar mantle that are probably quite fertile. For example, the REE pattern of the A15 Green Glass is rather flat. It is not chondritic and has a small negative Eu anomaly, but it is not strongly depleted in the LREE. This would make it more fertile than modern-day MORB mantle. Therefore, models of lunar differentiation must accommodate a wide range of incompatible element depletions. Note that the A15 Green is not KREEPy; so REE abundances were not established by a late-stage mantle overturn.

Mars. Mars differentiated early into core, mantle, and crust. This is established by the significant ^{182}W anomalies in martian meteorites. Like mare basalts and unlike eucrites, martian basalts all come from depleted source regions and it is inferred that this depletion also occurred very early.

There are at least two varieties of martian mantles: one that produced the nakhlites and chassignites and another that produced the shergotttites. In particular, the shergottitte mantle is so depleted that it is difficult

to understand how shergottite basalt generation occurs. In one model-dependent (but internally consistent) model, the nakhlite source region is twice as depleted in incompatibles as the terrestrial MORB mantle; and the shergottite mantle is three times more depleted still.

There is great similarity between the Lu-Hf and Sm-Nd systematics of shergottites on the one hand and high-Ti mare basalts and KREEP on the other. This suggests that, if the Moon went through a magma ocean stage, so did Mars.

The redox state of the martian mantle is not known precisely. However, Fe-Ti oxide assemblages in the most primitive shergottites [i.e., those with the highest initial ε(Nd)] indicate an oxygen fugacity of ~IW. And the similarity of FeO contents in basalts from the Moon, Mars and the EPB indicates that all three of these bodies were at ~IW-1 at the time of core formation. And the shergottite mantle is near that value.

Because there are correlations between redox state and ε(Nd) within the shergottite suite, I believe the most oxidized shergottites have been influenced by crustal contamination. If so, then the martian crust is more oxidized than the martian mantle (~QFM).

The redox state of the nakhlite/chassignite mantle may also be more oxidizing. Wadhwa found no Eu anomaly in Nakhla clinopyroxenes; but Nakamura did. Wadhwa also found Eu anomalies in clinopyroxene from Chassigny. Therefore, the redox state of the nakhlite/chassignite mantle is uncertain. Even so, the similarity between the FeO contents of nakhlites and shergottites suggests that at the time of core formation, differences in redox states could not have been large.

Part of our uncertainty about nakhlites stems from the complex history of the nakhlite mantle. Comparison of the short- and long-lived chronometers in the Sm-Nd system indicates that, at some time in the past (~4 b.y.), the nakhlite mantle was refertilized. This is tricky and difficult to do, suggesting a differentiation event internal to the nakhlite mantle.

In summary, Mars differentiated very early into reservoirs that still exist today. The petrology of the martian mantle is complex but maybe less so than that of the Moon. The variation in redox state on Mars is, however, more complex than on the Moon.

Earth. Of course, the most complex planet of all is the Earth. And because of that, a great deal of its earliest history has been erased. Therefore, oddly, though we know more about the Earth than any other planet, it's earliest conditions are murky.

The Earth differentiated early to form a core. Tera has argued that this event occurred at 4.54 b.y. However, the arguments are complex to the non-plumbologist. But, if so, this predates the formation of the mare basalt source regions by ~100 m.y. However, such an age may be consistent with the discovery of a small (~2ε) ^{182}W anomaly in terrestrial rocks. Although if the core formed early, it is unclear why the W anomaly is not larger. Presumably either the core formed later than 4.54 b.y. or nonradiogenic chondritic W was added after core formation. In the latter case, it is unclear why this event is not recorded in the Pb system (i.e., why isn't the Pb age of the Earth younger?).

The redox state of the Earth is much more complicated than any other planet and is much beyond the scope of this abstract. There is an apparent paradox in that terrestrial rocks have less FeO than their extraterrestrial counterparts (~8 wt.% FeO). Taken at face value this means that core formation occurred under more reducing conditions (~IW-2.5). Yet, mantle rocks have oxygen fugacities of ~QFM. How can these observations be reconciled?

Venus and the Earth have similar FeO contents, so there is a strong possibility that planet size (i.e., pressure) plays a role. Recent experiments, in fact, suggest that FeO may disproportionate into Fe metal and Fe^{3+} at pressures as low as ~250 kbar. If metal produced in this way segregates to the core, this could explain both the high-fo2 of the upper mantle and its low FeO content. Further, thermodynamic calculations indicate that low pressure (< 30 kbar) pyrolite mineral assemblages at QFM would become more consistent with IW at higher pressures. Again, the main difference between Earth/Venus and the other terrestrial planets is size.

The extent to which the Earth has been differentiated is unclear. Oceanic basalts often have elevated $^{3}He/^{4}He$ ratios and solar Ne, suggestive of primoridial signatures. In addition, fertile spinel lherzolites from continental lithospheres may show little evidence of substantial melt removal (i.e., they are still lherzolites). On the other hand, no mantle reservoir yet sampled has a chondritic Nb/U ratio, as expected for undifferentiated mantle. These observations, taken as a whole, argue for extensive but incomplete differentiation. A corollary of these observations is that there is no terrestrial evidence for a magma ocean (unlike the case of the Moon/Mars) or for a Moon-forming giant impact.

Another peculiarity of the Earth is that material has been returned to the mantle via subduction tectonics. This has allowed the transport of hydrous minerals to the mantle, which would otherwise be dry (like the other terrestrial planets).

And because the Earth has abundant surficial water, it may be the only planet with granitoid continents. Tonalites, the main component of ancient continental shields, are formed by the partial melting of altered (i.e., hydrated basalts).

ACCRETION AND CORE FORMATION OF TERRESTRIAL PLANETS: INSIGHTS FROM EXPERIMENTALLY DETERMINED SOLUBILITY BEHAVIOR OF SIDEROPHILE ELEMENTS IN SILICATE LIQUIDS. Ph. Kegler[1,2], A. Holzheid[2,] and H. Palme[1], [1]Universität Köln, Institut für Geologie und Mineralogie, 50674 Köln, Germany, philip.kegler@uni-koeln.de, herbert.palme@uni-koeln.de, [2]Universität Münster, Institut für Mineralogie, 48149 Münster, Germany, holzheid@uni-muenster.de.

Introduction: In common models of core formation in the terrestrial planets the proto-planet is covered with a deep, hot and turbulent convecting magma ocean [e.g., 1]. Molten metal droplets of the accreted material sink through the partially or completely molten silicates to the bottom of the magma ocean, where the final equilibration with the mantle-silicates occur. Increasing amounts of accumulated metal at the bottom of the magma ocean leads to the formation of large metal diapirs, which will eventually become gravitationally instable and rapidly sink down to the centre of the planet contributing to the growth of the core [e.g.,2]. This leads to a strong partitioning of siderophile elements (e.g., Fe, Ni, Co, Ge, noble metals) as well as the chalcophile elements (e.g., Cu, Pb, Zn) into the core and a corresponding depletion n the mantle [3]. The trace amounts of siderophile and chalcophile elements that are retained in mantle silicates record the conditions of metal segregation. Moreover, if metal and/or metal sulfide segregation was an equilibrium process, the relative depletions of siderophile and chalcophile elements give important clues for deducing the conditions of differentiation and core formation processes in the Earth and other planetary bodies. The concentrations of many siderophile elements (e.g., Ni, Co, Ge, highly siderophile elements) are overabundant in the Earth's mantle compared to expected concentrations based on experimentally determined metal-silicate partition coefficients at one atmosphere. To explain this poor match between the experimental determined metal-silicate partition coefficients and observed abundances of the siderophile as well as some chalcophile elements in today's mantle, a strong temperature and pressure dependence is assumed for these elements and has been experimentally verified for some elements (summarized in [1]). According to [4-9] metal-silicate partition coefficients of Ni and Co converge at high pressure. Based on the convergence, the relative abundances of Ni and Co would be consistent with metal-silicate equilibrium at the base of a single stage magma ocean at a depth of about 800 km. The results of recent experiments showed a more complex behavior of Ni and Co metal-silicate partition coefficients with increasing pressure that does not support the single stage magma ocean model [10,11]. In addition kinetic constraints on metal-silicate separation scenarios, proposed by [12], question the model of metal-silicate equilibrium at the base of a magma ocean. To better understand possible metal-silicate equilibration within the magma ocean (and not limited to the base of the magma ocean) we have expanded our study to Ge and Cu by experimentally determining the metal-silicate partitioning of the two elements at elevated pressure.

Experimental and analytical methodology: Experiments were done within the range of 1 atm to 25 GPa at temperatures between 1300 and 2300°C. The experiments were performed with vertical gas mixing furnaces at the Universität Köln (1 atm), by using piston cylinder apparati at the Universität Münster and at the Bayerisches Geoinstitut (0.3-3.5 GPa) and by using multi anvil presses at the Bayerisches Geoinstitut (3.5-10 GPa). In all experiments either $Fe_{54}Ni_{29}Co_{17}$, $Fe_{97}Ge_3$, or $Fe_{97}Cu_3$ alloys were equilibrated with a synthetic basaltic melt (SiO_2: 49.1 wt.%; Al_2O_3: 14.1%; CaO: 24.9 %; MgO: 10.6 %; FeO: 7.0 %). The experiments were terminated by withdrawing the samples from the hot spot position into the cooling jacket position of the vertical gas mixing furnaces (1-atm experiments). The high pressure experiments were terminated by turning-off the power to the graphite heater (piston cylinder experiments) or $LaCrO_3$ heater (multi anvil experiments). All experimental charges were mounted in epoxy, cut longitudinally through the center of the assemblies and polished as microprobe sections. Metal phases and major elements of the silicate phases of the post-run charges were analyzed using a Jeol 8900RL electron microprobe (Universität Köln). Operating conditions for metal phases were 20 kV and 25 nA and a focused beam. Counting times were 60 sec. Major elements of the silicate phases were analyzed with 20 kV, 50 nA and a defocused beam (raster size 20 μm). Counting times were 60 sec. Trace elements, such as Ni and Co in the silicate phases were determined by electron microprobe with 20 kV, 400 nA and a defocused beam (raster size 20 μm). Counting times were up to 600 sec, giving detection limits of 50 ppm for NiO and CoO. Trace elements of Ge and Cu in the silicate phases were analyzed using a laser ablation ICP mass spectrometer (UP193HE - New Wave Research, Element 2 MS - Finnigan, Universität Münster). Meas-

ured isotopes were Ge73, Cu63, and – as internal standard - Ca44. The following conditions were used: energy density ~8.5 J/cm^2, pulse rate: 5 Hz, number of shots per single analysis: 100, spot size: 180 µm. The minimum detection limits (99% confidence) were 0.03 ppm for Ge and 0.01 ppm for Cu.

Results and discussion: In Figure 1 metal-silicate partition coefficients, $D^{met/sil}$, are plotted as function of pressure. All partition coefficients are recalculated to equilibrium with pure metals,(see [13] for more details). Appropriate activity coefficients of [14] (Ni, Co), [15] (Cu), and [16] (Ge) are used for calculation of $D^{met/sil}$. For better comparison, all plotted $D^{met/sil}$ values were additionally recalculated to an oxygen fugacity relevant for metal/silicate separation during core formation (-2.3 log units below the iron-wüstite buffer) by assuming NiO, CoO, GeO and Cu_2O as stable species in the silicate phases. Due to the lack of precise knowledge of temperature dependences of Cu and Ge $D^{met/sil}$ at elevated pressure, Ni and Co $D^{met/sil}$ were recalculated to 1450°C, i.e., run temperature of all Cu and Ge high pressure experiments. The main results of our study on metal-silicate partition coefficients can be summarized as follows : (1) $D^{met/sil}$ of Ni, Co, Ge, and Cu decrease with increasing pressure at constant temperature and IW-2.3. (2) Ni and Co $D^{met/sil}$ values change their pressure dependence from a strong dependence at pressures below 5 GPa to a weaker dependence at higher pressures. Identical values of $D^{met/sil}$ of Ni and Co, required to explain the chondritic Ni/Co ratio in the Earth mantle, are extremely unlikely within the pressure range of the upper mantle. (3) Co $D^{met/sil}$ is in agreement with the core-mantle ratio of Co at about 40 GPa. However, $D^{met/sil}$ values of Ni, Ge, and Cu at 40 GPa differ by factors of about 2, 5, and 7, respectively. Although the absolute abundance of Co in the Earth mantle could be the result of metal-silicate equilibration at the bottom of a 1200 km deep magma ocean, expected mantle contents of the other studied siderophile elements at 40 GPa would have reached only 15 % (Cu), 20 % (Ge), and 50 % (Ni) of the observed mantle abundances. Our observations question the hypothesis of a simple single stage magma ocean. Alternative hypotheses to explain the siderophile element abundances in the Earth mantle could be inefficient core formation [17], heterogeneous accretion [18,19], or self oxidation of the Earth mantle with a multiple stage magma ocean [20,21].

References: [1] Walter, M. J., et al. (2000) In: *Origin of the Earth and Moon*, pp 265-290. [2] Stevenson, D. J. (1990) In: *Origin of the Earth*, pp 231-249. [3] O´Neill, H. St. C. and Palme, H. (1997) In: *The Earth's mantle: Structure, composition and evolution* pp 3-126. [4] Li, J. & Agee, C. (1996) *Nature*, **381**, 686-689. [5] Li, J. & Agee, C. B. (2001). *GCA*, **65**, 1821-1832. [6] Bouhifd, M. A. & Jephcoat, A. P. (2003) *EPSL*, **209**, 245-255. [7] Tschauner, O. et al. (1999) *Nature*, **398**, 604-607. [8] Righter, K. & Drake, M. J. (2004) In: *Geochemistry of the mantle and core*, pp 425-449. [9] Chabot, N. L. et al. (2005) *GCA*, **69**, 2141-2151. [10] Kegler, Ph. et al. (2004) *LPSC XXXV*, 1632. [11] Kegler, Ph. et al. (2005) *LPSC XXXVI*, 2030. [12] Rubie, D. C., et al. (2003) *EPSL*, **205**, 239-255 [13] Holzheid, A. & Palme, H. (1996) *GCA*, **60**, 1181-1193. [14] Guillermet A.F. (1989) *Calphad* **13**, 1-22 [15] Maruyama, N. & Banya, S. (1980) *J. Jpn. Inst. Metals*, **44**, 1422-1431. [16] de Boer, F. R. et al. (1989) *Cohesion and Structure*. [17] Jones, J. H. & Drake, M. J. (1986) *Nature*, **322**, 221-228. [18] Ringwood, A. E. (1984) *Proc. R. Soc. London*, ***A395***, 1-46. [19] Wänke, H. et al. (1984) In: *Archean geochemistry*, pp 1-24. [20] Frost, D. J. et al. (2004) *Nature*, **428**, 409-412. [21] Wade, J. & Wood, B. (2005) *EPSL*, **236**, 78-95.

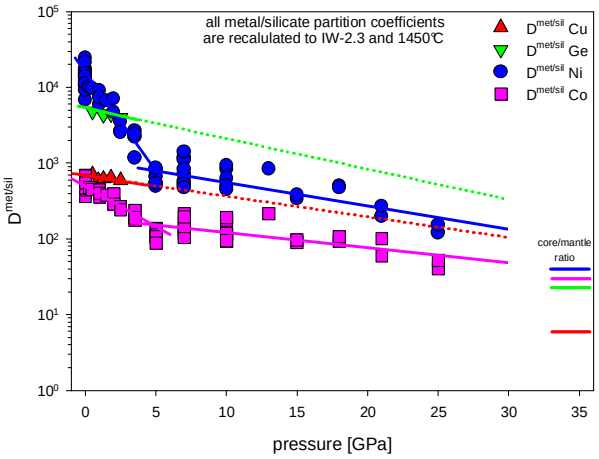

Figure 1: Metal-silicate partition coefficients of Cu, Ge, Ni, and Co vs. pressure. All data are recalculated to an oxygen fugacity 2.3 log units below the iron-wüstite buffer and 1450°C. The horizonal bars represent the core/mantle ratios in today's Earth (blue = Ni (39); pink = Co (31); green = Ge (26); red = Cu (6)).

WHAT CONTROLLED THE RATE OF CRUSTAL DIFFERENTIATION ON EARLY MARS?

Walter S. Kiefer and Qingsong Li, Lunar and Planetary Institute, 3600 Bay Area Blvd., Houston TX 77058, kiefer@lpi.usra.edu, http://www.lpi.usra.edu/science/kiefer/home.html, li@lpi.usra.edu .

Introduction

The crust of Mars is estimated to have a mean thickness of 45-62 km [1,2], corresponding to a volume of $6.4\text{-}8.8 \cdot 10^9$ km^3. For plausible values of the core radius, the crust is 4-6% of the silicate volume of the planet. Studies of the short-lived radioactive isotope systems ^{146}Sm-^{142}Nd and ^{182}Hf-^{182}W in the martian meteorites indicate that significant crustal differentiation occurred within the first few tens of millions of years after Mars accreted [e.g., 3-6]. However, this result is based on a limited number of martian meteorites, whose young igneous ages [7] suggest that they all originated in the Tharsis and Elysium volcanic complexes. Because the martian meteorites constitute a limited geographic sampling of the planet, they may not fully define the early isotopic evolution and differentiation history of Mars.

An alternative constraint on early crustal formation rates comes from cratering ages. A major feature of the global crustal structure of Mars is the hemispheric dichotomy [2]. The observed crater density indicates that the hemispheric dichotomy, and thus the underlying crust, was in place by 4.1 Ga [8]. Although there are significant uncertainties in our knowledge of the crater production rate on Mars [9], the dichotomy is certainly older than the Isidis impact basin, which is the youngest large basin on Mars. Assuming that the youngest basins on the Moon [10] and Mars have similar ages, most of the martian crust was certainly in place by 3.8 Ga.

Taken together, these results imply that the average crustal production rate was at least 9-17 km^3 yr^{-1} during the first 500-700 million years of martian history. The production rate shortly after Mars formed must have been higher yet, perhaps by an order of magnitude or more. On the other hand, the more recent crustal production rate has been much lower. If we assume that no more than 10% of the total crustal volume was produced after 3.8 Ga, then the mean crustal production rate in this interval was less than 0.25 km^3 yr^{-1}. Understanding early crustal differentiation on Mars thus requires understanding both the processes that controlled the high early crustal production rate and the processes that controlled the transition to a much lower rate.

Magma Ocean Models

Isotopic observations of the martian meteorites indicate that Mars accreted and at least partially differentiated within a few tens of millions of years. The energy released during rapid accretion and core formation may lead to at least partial melting of Mars, although thermal modeling of martian accretion suggests that such melting will not necessarily be global in extent [11]. Large-scale early melting of Mars would constitute a magma ocean, similar to that which occurred on the Moon [e.g., 12]. Following solidification of the magma ocean, gravitational overturning of the magma ocean cumulates could produce a crust with a volume that is consistent with observations [13]. Magma ocean crystallization products can also explain a variety of geochemical observations of the martian meteorites [14]. A significant concern about magma ocean models for Mars involves the mantle density. The predicted crystallization and overturn sequence results in a density of the uppermost mantle of 3100-3200 kg m^{-3} [13,15]. However, the chemical composition of the martian upper mantle is constrained by the composition of the martian meteorites and implies an upper mantle density of 3400-3500 kg m^{-3} [16]. Although magma ocean models for Mars deserve additional development, this mismatch between meteorite observations and theoretical magma ocean predictions suggests that some of the assumptions in existing magma ocean models are not correct.

Pressure Release Melting Models

As an alternative, we consider the possibility that some or all of the martian crust was produced by pressure release melting in a thermally convecting mantle. Previous studies of this process in early Mars have been performed using parameterized convection [17-20]. Parameterized convection models are one-dimensional (vertical

only) and thus yield only a solution for the average mantle temperature as a function of depth. However, melting is limited to regions with the highest temperatures. Parameterized convection simulations therefore require arbitrary assumptions about either melting efficiency or the magnitude of lateral variations in mantle temperature in order to make predictions about the magmatic history of a planet.

We avoid the limitations of parameterized convection by extending the spherical axisymmetric finite element convection simulations of Kiefer [21] to radioactive heating rates [22] appropriate for 4-4.5 Ga. The high Rayleigh numbers appropriate for early Mars (10^8-10^9) require high grid resolution (6.6 km in this study) to properly resolve the narrow thermal boundary layers. Melting is calculated with respect to the solidus of the Bertka and Holloway [23] Mars mantle composition.

Partitioning of Radioactivity into the Crust

Current geochemical and geophysical estimates are that roughly half of the radioactive elements on Mars have now been partitioned into the crust (see summary in [21]). Removing heat production from the mantle contributes to mantle cooling and thus decreases the magnitude of future magmatic activity. As a test of the importance of this effect, we have compared the magma production in two models. In the first, heat production is homogeneously distributed throughout the crust and mantle at a level appropriate for earliest Mars. In the second, we simulate early crustal production by instantaneously moving 50% of the radioactive heating from the mantle to the crust. After integrating forward in time for 500 million years, the second model has an average internal temperature that is 40 K lower than the first model. The average melt production in the second model is 50% of that in the first model. We conclude that this effect plays only a small role in the overall reduction of the crustal production rate during early martian evolution.

Loss of Mantle Water

Observations of the martian meteorites indicate that the martian mantle may contain several hundred ppm of water [24]. Water is relatively incompatible and should be carried to the crust during melting. Even a loss of 50 ppm water from the mantle can change the solidus by 100 K at low pressure [25], which results in nearly an order of magnitude reduction in the melt production rate. Additional water loss is possible and would cause further reduction in the melt production rate. Our current results suggest that loss of water from the mantle may be an important contributor in explaining the rapid decrease in crustal production on early Mars. The effects of the possible transition from a mobile surface layer to stagnant lid convection [26] on magma production rates also needs further exploration.

References [1] Wieczorek and Zuber, JGR 109, E01009, doi:10.1029/2003JE002153, 2004.[2] Neumann et al., JGR 109, E08002, doi:10.1029/2004JE002262, 2004. [3] Harper et al., Science 267, 213-217, 1995. [4] Halliday et al., Space Sci. Rev. 96, 197-230, 2001. [5] Kleine et al., Geochim. Cosmochim. Acta 68, 2935-2946, 2004. [6] Foley et al., Geochim. Cosmochim. Acta 69, 4557-4571, 2005. [7] Nyquist et al., Space Sci. Rev. 96, 105-164, 2001. [8] Frey, JGR 111, E08S91, doi:10.1029/2005JE002449, 2006. [9] Hartmann and Neukum, Space Sci. Rev. 96, 165-194, 2001. [10] Dalrymple and Ryder, JGR 98, 13,085-13,095, 1993. [11] Senshu et al., JGR 107, doi:10.1029/2001JE001819, 2002. [12] Shearer et al., pp. 365-518 in *New Views of the Moon*, Reviews in Mineralogy and Geochemistry, vol. 60, 2006. [13] Elkins-Tanton et al., JGR 110, E12S01, doi:10.1029/2005JE002480, 2005. [14] Borg and Draper, Meteoritics Planet. Sci. 38, 1713-1731, 2003. [15] Elkins-Tanton et al., Meteoritics Planet. Sci. 38, 1753-1771, 2003. [16] Bertka and Fei, Earth Planet. Sci. Lett. 157, 79-88, 1998. [17] Weizman et al., Icarus 150, 195-205, 2001. [18] Hauck and Phillips, JGR 107, doi:10.1029/2001JE001801, 2002. [19] Breuer and Spohn, JGR 108, doi:10.1029/2002JE001999, 2003. [20] Breuer and Spohn, Planet. Space Sci. 54, 153-169, 2006. [21] Kiefer, Meteoritics Planet. Sci. 38, 1815-1832, 2003. [22] Wänke and Dreibus, Phil. Trans. R. Soc. A349, 285-293, 1994. [23] Bertka and Holloway, Contrib. Mineralogy Petrology 115, 313-322, 1994. [24] Leshin et al., Geochim. Cosmochim. Acta 60, 2535-2650, 1996. [25] Asimow et al., Geochem. Geophys. Geosys.5, Q01E16, doi:10.1209/2003GC000568. [26] Nimmo and Stevenson, JGR 105, 11,969-11,978, 2000.

TUNGSTEN ISOTOPE CONSTRAINTS ON CORE FORMATION IN TERRESTRIAL PLANETS.

T. Kleine[1], [1]Isotope Geochemistry and Mineral Resources, ETH Zurich, Switzerland (kleine@erdw.ethz.ch).

Introduction: Planetary accretion and core formation are intimately linked. As a planet grows, gravitational energy is deposited and the interior heats up, leading to melting and separation of dense metal melts that sink to the centre and form a core. Determining the timing of core formation thus will provide age constraints on accretion. The ^{182}Hf–^{182}W chronometer is well suited to date core formation in planetary bodies because (i) the life-time of ^{182}Hf is similar to the anticipated accretion timescales of terrestrial planets, (ii) siderophile W fractionates from lithophile Hf during metal segregation, and (iii) Hf and W are refractory and occur in chondritic (and hence known) proportions in bulk planetary bodies.

The W isotope evolution of chondrites is an important reference in Hf-W chronometry because it is representative for the bulk planet; it is defined by the present day ^{182}W/^{184}W of chondrites and the initial ^{182}Hf/^{180}Hf of the solar system. These parameters are $\varepsilon_W = -1.9\pm0.1$ ([1-4]; ε_W is the deviation of ^{182}W/^{184}W from the terrestrial value in parts per 10^4) and ^{182}Hf/^{180}Hf $\sim1\times10^{-4}$ [1,3,5]. If core formation occurred when ^{182}Hf was extant, then the mantle (with its high Hf/W) will evolve to $\varepsilon_W>-1.9$, whereas the core (with its Hf/W~0) will maintain its W isotope composition of $\varepsilon_W<-1.9$ acquired at the time of core formation. Tungsten isotope data for differentiated meteorites are consistent with such a pattern. Most magmatic iron meteorites have ε_W values between –4 and –3 [5-9], indicating that core formation in their parent bodies occurred in less than 1.5 Myr after the start of the solar system. Radiogenic W isotopes in eucrites (ε_W up to ~40) result from an early depletion of W in eucrites (Hf/W~30) and indicate differentiation in less than ~5 Myr [4].

Core formation in Mars: All Martian meteorites exhibit radiogenic ε_W relative to chondrites [4,10]. Nakhlites are more radiogenic than shergottites, probably reflecting Hf-W fractionation during early mantle differentiation. This is consistent with the presence of ^{142}Nd anomalies in nakhlites [11]. Shergottites may best represent the ^{182}W/^{184}W of the bulk Martian mantle because their ^{142}Nd/^{144}Nd it close to chondritic [4,10]. Owing to uncertainties in the Hf/W ratio of the Martian mantle the calculated Hf-W ages for core formation vary between 0 and 12 Myr.

Accretion and differentiation of the Earth and Moon: The W isotope composition of Earth's mantle is more radiogenic than chondrites., indicating that core formation at least in part occurred during the life-time of ^{182}Hf. Assuming that Earth's core formed instantaneously, a Hf-W model age of ~30 Myr is calculated [1-3]. Accretion of Earth however was a protracted process. If Earth accreted at an exponentially decreasing rate and W isotope equilibrium during core formation was always achieved, then accretion terminated at ~50 Myr [3,13]. The real accretion process for Earth-mass bodies however involved the delivery of large masses of core material at different times. The effects on the W isotope evolution of Earth's mantle will then largely depend on the differentiation history of the impacting objects and the degree of W isotope equilibration between incoming material and Earth's mantle. Both of these parameters are not known but are critical for calculating Hf-W ages. For instance, early core formation with complete metal-silicate equilibration and late core formation with only limited equilibration can result in the same W isotope composition of Earth's mantle [12-15]. Although this limits the application of Hf-W as a chronometer for core formation, W isotopes can be used to constrain the conditions of metal-silicate separation in Earth's mantle. This requires the timing of core formation to be determined independently.

The age of the Moon provides the timing of the last major accretion stage in Earth's history and as such likely provides the time at which Earth's core had entirely been separated. Using the crystallization age of the lunar magma ocean of 30-50 Myr as the age of the Moon (and hence the giant impact) [16], it can be shown that most of the incoming W equilibrated with the mantle before entering Earth's core. However, W isotopes cannot constrain the degree of equilibration during the giant impact and would be consistent with both complete and absent re-equilibration of the impactor's core with Earth's mantle. The overall high degree of metal-silicate equilibration during core formation suggests that core formation occurred by the physical separation of small metal droplets from molten silicate in a magma ocean.

References: [1] Kleine T. et al. (2002), *Nature*, *418*, 952-955. [2] Schoenberg R. et al. (2002), *GCA*, *66*, 3151-3160. [3] Yin Q.Z. et al. (2002), *Nature*, *418*, 949-952. [4] Kleine T. et al. (2004), *GCA*, *68*, 2935-2946. [5] Kleine T. et al. (2005), *GCA*, *69*, 5805-5818. [6] Horan M.F. et al. (1998), *GCA*, *62*, 545-554. [7] Lee D.C. (2005), *EPSL*, *237*, 21-32. [8] Markowski A. et al. (2006), *EPSL*, *242*, 1-15. [9] Schérsten A. et al. (2006), *EPSL*, *241*, 530-542. [10] Foley C.N. et al. (2005), *GCA*, *69*, 4557-4571. [11] Harper C.L. et al. (1995), *Science*, *267*, 213-217. [12] Halliday A.N. (2004), *Nature*, *427*, 505-509. [13] Kleine T. et al. (2004), *EPSL*, *228*, 109-123. [14] Jacobsen S.B. (2005), *AREPS*, *33*, 531-570. [15] Nimmo F. and Agnor C.B. (2006), *EPSL*, *243*, 26-43. [16] Kleine T. et al. (2005), *Science*, *310*, 1671-1674.

WAVE WARPING AS A REASON (IMPETUS) OF DENSITY (CHEMISTRY) DIFFERENTIATION OF PLANETS AT VERY EARLY STAGES OF THEIR FORMATION.

G.G. Kochemasov, IGEM of the Russian Academy of Sciences, 35 Staromonetny, 119017 Moscow, Russia, kochem@igem.ru

The comparative wave planetology starting from a notion that "orbits make structures" comes to 4 theorems of planetary tectonics: 1) Celestial bodies are dichotomic, 2) Celestial bodies are sectoral, 3) Celestial bodies are granular, 4) Angular momenta of different levels blocks tend to be equal [1, 2, 3 & others]. Why orbits make structures? Because two fundamental properties of all celestial bodies (from a small asteroid to giant stars –asters and to super galaxies) are their motion and rotation. Moving in keplerian non-round (elliptic, parabolic) orbits with periodically changing accelerations masses of celestial bodies experiment oscillations or warpings. These waves have stationary character and 4 directions (ortho- and diagonal). Their interference produces uprising (+), subsiding (-) and neutral compensated (0) blocks size of which depends on warping wavelengths. All starts with the fundamental wave 1 long $2\pi R$ that is an obvious reason for the ubiquitous tectonic dichotomy – an opposition of the risen hemisphere and the fallen one (Theorem 1). The best examples: Earth, Mars, Iapetus, asteroids. The wave 1 has overtones and the most prominent wave 2 long πR produces sectors combined into structural octahedron (Theorem 2). This figure or its parts are easier seen in shapes of small bodies not affected by stronger gravity of larger bodies. A "perfect" diamond shape was firstly noted in outlines of Amalthea, then in some other small bodies. The larger bodies like Earth, Mars, Venus demonstrate some faces-sectors and vertexes of this structure.

Along with above common for all bodies structures every body is also warped by individual waves lengths of which is strictly dependent on orbital frequencies: higher frequency – tighter wave spacing, lower frequency – wider wave spacing. These intersecting waves produce tectonic granules. Their sizes, accordingly, increase inversely proportional to orbital frequencies: the Sun's photosphere $\pi R/60$, Mercury $\pi R/16$, Venus $\pi R/6$, Earth $\pi R/4$, Mars $\pi R/2$, asteroids $\pi R/1$(Fig. 1). With increasing solar distance in planets increase the relief range, density of lowland basalts (judged by Fe/Si and Fe/Mg in them), density difference between lowland and highland materials (required by Theorem 4) (Fig. 2).

All mentioned wave forms: $2\pi R$-structures, πR-structures, individual wave ($\pi R/60 – \pi R/1$) structures are superimposed in celestial spheres producing rather complex shapes. On the whole, up to Earth overall shapes are nearly spherical bur Mars already has an elliptical shape and asteroids oblong convexo-concave shapes (Fig. 1). In Fig. 3 are shown described wave forms observed in the solar photosphere mainly by the SOHO. Sun's dichotomy at the moment of imaging is of the martian type – north-south segmentation; dark sectors are very contrasted; supergranules are known from the thirties of the 20th century, long before they were recognized in planetary spheres. These series of images shows that the wave shaping concerns all celestial bodies including stars and their descendants –planets.

All these wave shapings started to act in the very earlier periods of planetary formation when orbits were much more elongated, periodic changes in accelerations more sharp and thus warping inertia-gravity forces more important. Planets still kept much of their primordial volatiles that helped to differentiate spheres into core, mantle and crust. There is a semi-quantitative dependence between orbital frequencies and a rate of volatile wiping out of planets [4]. Thus, Venus is more wiped of volatiles than Earth, and Mars is less outgassed than Earth. Titan with is orbital frequency 1/16 days is very strongly outgassed and continues to do so loosing its mass and shrinking (all its surface shows cross-cutting very tight waves – some take them for dunes). In atmospheres of three planets the ratio of radiogenic to primordial argon is increasing from Venus to Earth and to Mars (1, 300, 3000) confirming diminishing outgassing rate.

Rich in volatiles, H_2O martian mantle is easily differentiated producing enormous quantities of light (not dense) material for building high standing highland crust. This silicic alkaline poor in Fe material does not show very high Si (only upto 18- 21%, after "Odyssey") most probably due to significant admixture of light (not dense) salts. This admixture is necessary to diminish density of the highland crust building material required by the rule of the angular momentum equilibration (Theorem 4) (Fig. 2). Under this condition we do not see any significant difference between gravity signals over the northern and southern hemispheres so different in heights, colors, compositions. In this respect there is a significant difference between polar caps at south and north (sectors superimposed on segments). They cannot be similar fundamentally as they add mass to opposing tectonic blocks -sectors with different signs (northern polar uplift on subsided Vastitas Borealis and southern polar hollow). Indeed, the northern layered icy deposits are not only less voluminous but consist mainly of H_2O ice (specific gravity 0.92 g/cm^3); the southern layered icy deposits are not only more voluminous but consist of H_2O and CO_2 ices (specific gravity 1.56

g/cm^3). As a result the northern cap is more convex and the southern cap is more flat because carbon dioxide dry ice is more easily evaporated. But on the segmental scale regoliths of the northern lowlands are richer in the ground ice (additional mass) than the southern highlands.

Very light, probably consisting of albitites, syenites, granites crust in the south was predicted in 1995 before launching Pathfinder [5]. At this time a majority of planetologists believed in basaltic highland crust. The Pathfinder mission discovered andesites. Later on the THEMIS experiment of MGS detected dacites – more acid rocks. And now Dr. H.Y. McSween –a petrologist of the Spirit rover project came to a conclusion that on Mars there is an igneous alkaline province. Earlier we compared the Columbia Hills layered igneous sequence with one alkaline province at Earth – the alkaline massifs of Kola Peninsula: Lovozero and Khibiny. A recognition of alkaline rocks on another than Earth cosmic body (A.V Ivanov showed this by finding small fragment of a rock containing alkaline minerals in meteorite coming probably from Phobos [6]) opens a new perspective in planetology, cosmic petrology. An early planetary differentiation facilitated by volatiles and required by important wave warpings to equilibrate angular momenta of tectonic blocks with different planetary radii is a way to approach a problem of causes and mechanisms of this differentiation.

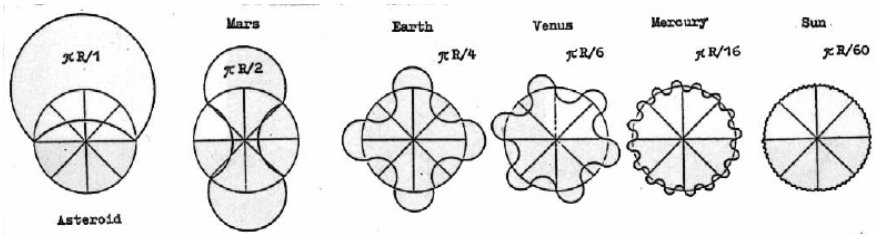

Fig.1 Geometrical representation of warping waves in celestial bodies [1]

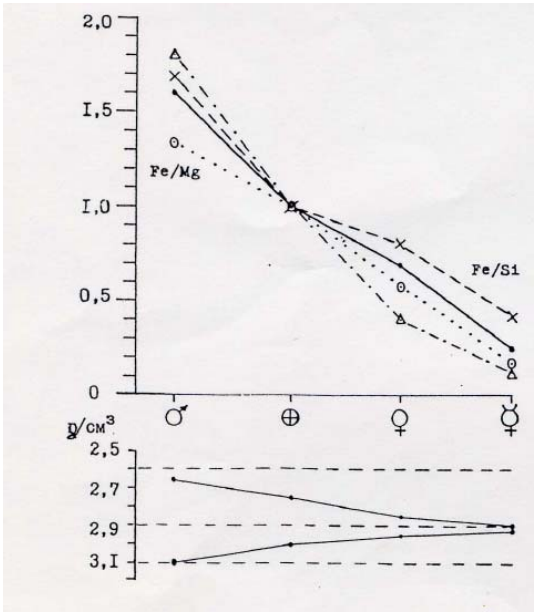

Fig. 2 Ratios of some planetary crust parameters compared to the terrestrial ones taken as 1:solid line – relief, dashed line – Fe/Si, dots – Fe/Mg in basalts of lowlands, dot-dashed line – highland/lowland density contrast. Below: increasing highland/lowland density contrast with increasing solar distance.[5].

References: [1] Kochemasov G. G. (1994) 20th Russian-American microsymposium on planetology. Abstr., Moscow, Vernadsky Inst., 46-47; **[2]** Kochemasov G. G. (1998) Proceedings of international symposium on new concepts in global tectonics ('98 TSUKUBA), Tsukuba, Japan, Nov. 1998, 144-147; **[3]** Kochemasov G. G. (1999) The Fifth International Conference on Mars, July 18-23, 1999, Pasadena, California. Abstr. # 6034. LPI contribution # 972. LPI, Houston, (CD-ROM); **[4]** Kochemasov G.G. (2006) 36th COSPAR Scientific Assembly, Beijing, China, 16-23 July 2006, abstr. COSPAR2006-A-00789,CD-ROM; **[5]** Kochemasov G. G. (1995) Golombek M.P., Edgett K.S., Rice J.W. Jr. (Eds). Mars Pathfinder Landing Site Workshop II: Characteristics of the Ares Vallis Region and Field trips to the Channeled Scabland, Washington. LPI Tech. Rpt. 95-01. Pt.1.LPI, Houston, 1995, 63 pp. **[6]** Ivanov A.V., Kononkova N.N., Yang S.V., Zolensky M.E.(2003) Meteoritics & Planetary Science, 2003, v.38, # 5, 725-737

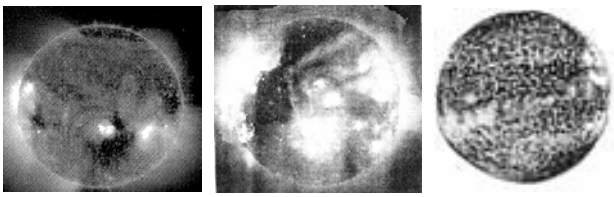

Fig. 3 Wave forms in the solar photosphere: dichotomy (N-S), sectoring, supergranulation

The Final Assemblage of Terrestrial Planets in the Solar System. D.N.C. Lin[1] ,Makiko Nagasawa[2], and E. Thommes[3] [1]Astronomy and Astrophysics Department, University of California, Santa Cruz, CA 95064 email: lin@ucolick.org, [2]National Astronomical Observatory of Japan, Mitaka, Tokyo, Japan, email: nagaswmk@cc.-nao.ac.jp, [3]Canadian Institute for Theoretical Astrophysics, University of Toronto, Toronto, Canada, email: thommes@cita.utoronto.ca

We consider the stage of gas depletion after the formation of a Jupiter-like planet in the disk. The gas depletion changes the gravitational potential and causes the sweeping of a secular resonance. We find that the secular resonance passes through the terrestrial region from outside to inside, that the resonance excites the eccentricities of isolated embryos, and that it leads to orbit crossing. Because the remnant disk is still present in this stage, the gas drag due to tidal interaction is still effective. The tidal drag effectively damps the eccentricities of the fully grown embryos. This process allows the system to form circular orbits analogous to our solar system. We also find that the tidal drag induces the decay of the semimajor axes of the embryos. As a result of balance between damping and excitation of eccentricity, the embryos migrate along with the secular resonance. This ``secular resonance trapping'' can lead to rapid collisions and mergers among the embryos as they migrate from the outer to the inner region, concurrent with the disk depletion. Since the induced migration is strongest near the Jovian orbit, the final terrestrial planets tend to be concentrated in a relatively small region (<2 AU). We suggest that this mechanism may be the origin of the severe present-day mass depletion of the asteroid belt. A natural implication of this scenario is that the terrestrial planets formed after the emergence of gas giants . The formation sequence proceeds with the asteroids followed by the final assemblage Mars within 10 Myr, the Earth on a timescale up to 30 Myr, and finally Venus at 50 Myrs. These results are consistent with the differential cosmochemical age estimates.

EARLY LUNAR DIFFERENTIATION: MIXING OF CUMULATES. John Longhi, Lamont-Doherty Earth Observatory, Palisades, NY 10964 (longhi@ldeo.columbia.edu)

The compositional patterns of Ni and Co in olivine from lunar rocks [1] are similarly peculiar, but qualitatively different. Modeling of magma ocean crystallization produces analogous patterns of Ni and Co [2], indicating that the basic compositional patterns were established during magma ocean crystallization. The modeling is carried a step further by applying the calculated mineral compositions to the cumulate mixing model for the green glass source region [3].

Fig. 1 illustrates Ni and Co ion probe data for lunar olivines from [1] and some Ni microprobe data from [4]. Although there is some within-group coherence (i.e., a negative correlation of concentration with Mg' (Mg/(Mg+Fe)), the overall patterns are unexpected within the most magnesian olivines showing unexpectedly low concentrations of Ni and Co. The patterns diverge in that the Ni pattern appears to have a peak (mare basalt olivine), whereas the Co pattern appears to increase monotonically.

These general patterns are reproduced by calculated Ni and Co concentrations in olivine and orthopyroxene using the partitioning model of [5] as applied to the crystallization of a magma ocean (Fig. 2) with initial bottom pressure of 3.0 GPa and bulk composition (LPUM) equal to Earth's upper mantle minus most of the alkalis [6]. With the possible exception of the ferroan anorthosites (FAN), lunar rocks do not form from the magma ocean, but their source regions do. Also, as Fig. 3 illustrates the calculated patterns appear different when plotted against Mg' in olivine as opposed to extent of crystallization.

Recent modeling of the major elements in the green glass (mare basalt) source region has shown that there is a restricted range of permissible source compositions with low AL2O3, but variable olivine/pyroxene ratio, that can produce the green volcanic glass compositions either by accumulated polybaric fractional fusion or batch melting [3]. Mass-balance calculations indicate that these source compositions are composites of intermediate (olivine + orthopyroxene) and late-stage cumulates (low- and high-Ca pyroxene± plagioclase) [3]. Figure 3 illustrates the major element mixing parameters for the olivine-rich end member (63% fo92, 37%a en56) applied to Ni and Co. The correspondence between the calculated source (solid rectangle labeled GGS) and the most magnesian Apollo 12 olivines is quite good. The source of the Mg-suite is unknown, but their petrogenesis involves mixing of KREEP at some stage [7], so mixing vectors to late-stage compositions are shown. Only small amounts of KREEP are necessary to produce the observed compositions of the Mg-suite, so Mg' of the Mg-suite source (MgS) is close to the cumulus mineral trend and Ni an Co concentrations must be higher, The simple FAN model (A) posits that the olivine should be equivalent to the magma ocean cumulus olivine at the Mg' of the natural olivines (0.65). The calculated FAN compositions have the correct dispositions relative to the natural compositions, but the calculated compositions are too high by a factor of 2 A more complicated model derives anorthosites by remelting overturned high-level mafic cumulates [6]. In this case (B), anorthosite olivines should have compositions close to the cumulus pyroxene trend.

These calculations are consistent with a magma ocean of terrestrial composition that encompassed most of the Moon. Overturn and mixing of cumulates are responsible for the mare basalt, Mg-suite, and ferroan anorthosite source regions.

REFERENCES: [1] Shearer C.K. and Papike J.J. (2005) *Geochim. Cosmochim. Acta 69*,3445-3461. [2] Longhi J. and D. Walker (2006) *Lunar and Planetary Science XXXVII,* Abstract #2452, Lunar and Planetary Institute, Houston. [3] Longhi J. (2006) in press *Geochim. Cosmochim. Acta*. [4] Ryder G. (1983) *LPI Tech.Rpt. 83-02,* 86-88.

[5] Jones J.H. in T.J. Ahrens (ed.), *Rock Physics and Phase Relations: a Handbook of physical Constants*,73-104. [6] Longhi J. (2003) *J. Geophys. Res., 108,* 10.1029/2002JE001941. [7] Warren P.W. (1983) *PLSC 8th*, 233-241.

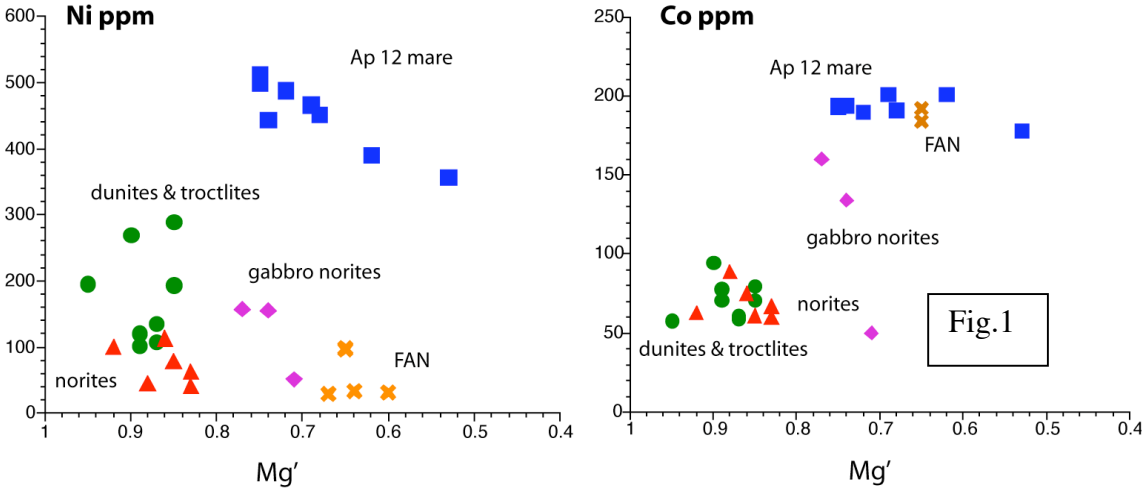

Fig.1

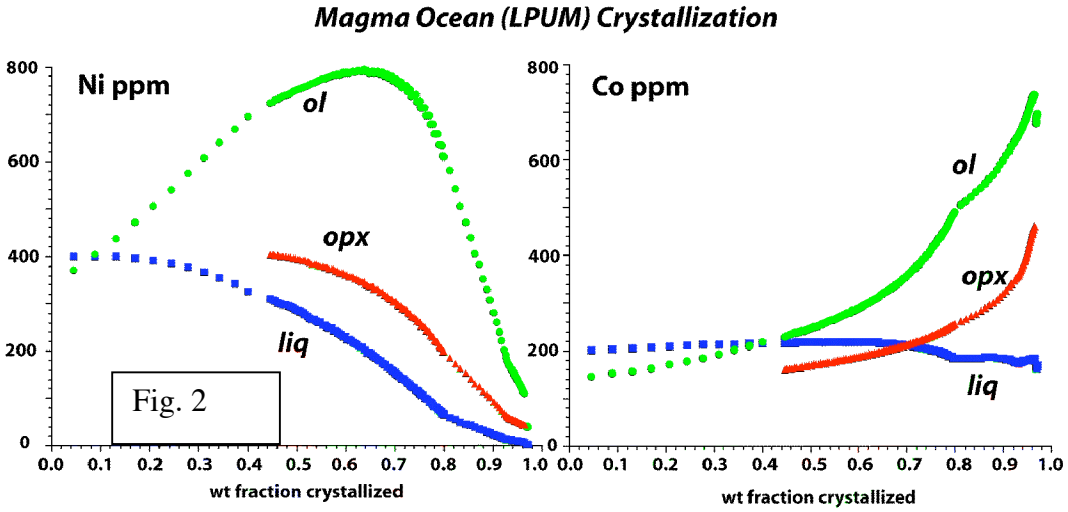

Fig. 2

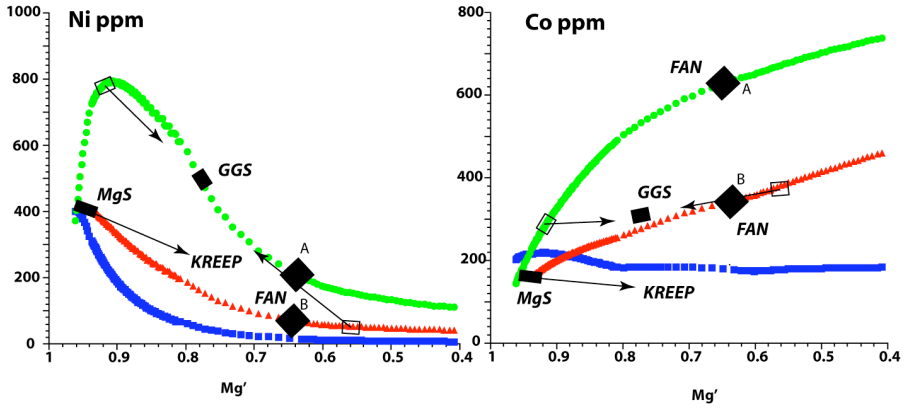

Fig. 3

DIFFERENTIATION OF THE GALILEAN SATELLITES: IT'S DIFFERENT OUT THERE. William B. McKinnon. Department of Earth and Planetary Sciences and McDonnell Center for the Space Sciences, Washington University, Saint Louis, MO 63130; mckinnon@wustl.edu.

Introduction: The internal structures of Jupiter's large moons — Io, Europa, Ganymede, and Callisto — can be usefully compared with those of the terrestrial planets, but it is evolutionary paths to differentiation (or in one case avoided) taken by these distant and divergent worlds that are in striking contrast to that presumed to have governed the terrestrial planets and differentiated asteroids. This talk will cover several aspects: 1) time scales; 2) the role of large impacts; and 3) long-term vs. short-term radiogenic heating. One conclusion is that iron core formation in large ice-rock satellites may in fact follow the classic Elsasser model.

Background. The large moons of Jupiter, Io, Europa, Ganymede, and Callisto, are all considered to be differentiated, although Callisto only partly so [1]. The evidence comes from interpretation of their second-degree gravity fields, as measured by *Galileo*, and assumes hydrostatic (though rotationally and tidally distorted) bodies. In the case of Ganymede independent corroboration comes from its intrinsic dipole magnetic field, which implies a dynamo in a liquid metallic core. Europa has an induced magnetic field, which is interpreted as requiring a conducting, saline aquasphere ("ocean") at depth — again consistent with a differentiated interior [2]. And Io is so intensely tidally heated that there is little question that it is a differentiated body. Only Callisto is deemed to be incompletely differentiated (~20–40% ice-rock separation), yet it too has an induced magnetic field and thus an internal aquasphere.

The terrestrial planets accreted over several 10s of Myr, based on the latest radiometric chronologies, and in doing so suffered catastrophically energetic impacts [e.g., 3]. Early magma oceans, if not global melting, must have resulted. Metal from rock differentiation in such an environment was facile. Even smaller asteroids were able to differentiate, apparently due to heat release due to the disintegration of short-term radionuclides, principally ^{26}Al and ^{60}Fe [e.g., 4]. Neither of the these mechanisms or processes can be called upon to explain the differentiation of the Galilean satellites, however, which in some ways recall earlier scientific ideas for planetary evolution.

Time Scales. The Galilean satellites are a byproduct of the formation of Jupiter. Jupiter formed within the lifetime of the gaseous solar nebula, which based on astronomical studies of nearby (analogous) protostars, had a lifetime in the 1–10 Myr range [e.g., 5; see 6]. The leading model for giant planet formation in our Solar System is the *core accretion–gas capture* model, in which a rock-ice-gas planet accretes by normal processes in the solar nebula until a mass threshold is crossed and nebular gas and entrained solids rapidly flow onto this planetary "core," inflating it to giant planet status [e.g., 7]. Under such circumstances the proto-giant planet may then open a gap in the solar nebula and terminate its accretion — or nearly so as nebular material continues to flow across the gap at a much reduced rate. An accretion disk forms about the nascent giant planet from this material, and satellites can then form (accrete) from this end-stage solar bequest, augmented by larger solar planetesimals that are captured into the disk [8,9].

As such, the accretion time scale for formation of the Galilean satellites is extended far beyond the intrinsic dynamical time scales in the protojovian disk. Accretion can last as long as the solar nebula exists to feed the protojovian disk, and as long as newly formed satellites can survive against gas drag and tidal-torque induced inward migration [8,9]. These time scales can be considerable (>1 Myr) for these so-called *gas-starved* accretion disks [8]. The solids entrained in the nebular flow across the gap would necessarily be relatively small, perhaps <1 m diameter [8], and should be compositionally representative of Jupiter's formation zone, and thus likely similar to the smaller carbonaceous bodies of the mid-to-outer asteroid belt (see [6,10] for discussion).

Extended formation times are required if bodies the size of the Galilean satellites (i.e., Callisto) are to form undifferentiated or nearly so. This gives sufficient time to radiate accretional energy to space (provided the accretional heat is not deeply buried). For the atmosphereless case, which applies to gas-starved accretion disks, the accretion time must exceed ~few x 10^5 yr [11]. While strictly speaking this argument applies only to Callisto, the gas-starved disk model posits that all the Galilean satellites grew more-or-less simultaneously, from a diminishing solar inflow [9], so they should have all formed on similar time scales, and thus likely accreted in relatively cool state. Cool is relative to the protojovian disk background, however, so Europa and especially Io should have seen somewhat elevated initial temperatures (but still well shy of rock or metal melting).

Large Impacts. By a similar argument, large, ice-melting impacts must be avoided in general, if Callisto is to emerge only partially differentiated. The Galilean

satellites ostensibly grew from the sweep up of smaller debris that entered jovian orbit from the outside, and so would not have experienced the violent end-stage accretion that affected the terrestrial planets (i.e., many large protoplanets on crossing orbits). Accretional velocities should have been close to satellite escape speed, which would have minimized accretional heating (all other things being equal). Accretion of smaller bodies also works in the right direction, but it is not clear if they were small enough. Even 10-m class bodies, accreting over 1 Myr, could bury a considerable amount of heat (this depends on the amount of impact stirring) [6]. Water ice is relatively easy to melt by shock [12], and late accreting ice-rock impactors on the Galilean satellites should have completely melted their ice fractions.

Short-lived Radiogenic Heating. Callisto again sets bounds, this time on the potential contribution of short-lived radiogenic heating to satellite evolution. If accretion began too early, then heat released by the decay of ^{26}Al and ^{60}Fe should have melted Callisto's ice fraction. Although one could take Callisto to be no more than 20% differentiated, a strict lower limit to Callisto's formation time presumes 100% ice melting. Starting from 100 K, and assuming an ^{60}Fe/^{56}Fe ratio between 2.8 x 10^{-7} and 10^{-6}, I find that Callisto *completed* its accretion no earlier than 2.6 to 3.0 Myr after t = 0 (CAI condensation in the inner solar nebula) [13]. While certainly compatible with the nebular time scales discussed above, the implication for the other satellites is that short-lived radiogenic heating is at best a modest early power source. The satellites of Jupiter were not driven to differentiate by short-lived radiogenics alone (unlike, say, Vesta, or the parent bodies of the metallic asteroids).

Discussion. If the power sources above were not sufficient, then differentiation of the Galilean satellites falls to long-lived radiogenic and tidal heating. There is no question that this would have been sufficient for Io and Europa, even without tidal heat, as the ice fraction in a uniform primordial Europa (25-30% by volume) would not have been great enough for solid-state ice convection and efficient heat transport (and ice buffering of internal temperatures is not even an issue for Io). For Ganymede the story is different, and if Callisto is only partially differentiated then explaining a differentiated Ganymede is more difficult. This is an old problem [14]. Establishment of the Laplace resonance between Io, Europa, and Ganymede later in Solar System history is a potential solution [15], but if the Laplace resonance is primordial [16], then Ganymede's present state (complete separation of ice from rock) has no obvious explanation. Nominally, a primordial origin for the resonance brings Io to the threshold of rock-metal differentiation (Fe-FeS eutectic melting) after the protojovian nebula dissipates [6] and pushes Europa well past the threshold. Enhanced tidal flexing and dissipation result.

Without tidal heating, long-term radiogenic heating should bring a rock-metal satellite interior from a cold start (~250 K) to the threshold of differentiation in ~1 Gyr [e.g., 2]. This may best apply to Ganymede, or Europa if the Laplace resonance is *not* primordial. Solar composition rock implies a S/(Fe + S) ratio by weight of 23% [17], close to the Fe-FeS eutectic (at appropriate pressures). The rocky component of these worlds is likely highly oxidized, however [18,19], implying relatively low Mg#s (by terrestrial standards), lower amounts of Fe metal available for core formation, or even oxidized Fe_3O_4 as a potential core component. The latter may be important, as an Fe-S-O melt wets silicate grains readily [20], and thus can easily percolate downward, Elsasser style, to form a core.

If the Fe-alloy melt is not oxygen-bearing, core formation is delayed until sufficient melt accumulates or solid-state silicate convection begins, in which melt can accumulate in deformation bands [e.g., 21]. Regardless, FeS is predicted to be the dominant metallic phase in the rocky component [see, e.g., 22], so complete "melt out" (100% core formation efficiency) may require internal temperatures to be overdriven by tidal heating. Ganymede, and possibly Europa, may retain residual FeS in their rock mantles.

References: [1] Schubert G. et al. (2004) in *Jupiter-The Planet, Satellites and Magnetosphere [JPSM]*, F. Bagenal et al., eds., CUP, 281-306. [2] Greeley R. et al. (2004) in *JPSM*, 329-362. [3] Canup R.M. and C.B. Agnor (2000) in *Origin of the Earth and Moon,* R.M. Canup and K. Righter, eds., Univ. Ariz. Press, 113-129. [4] Srinivasan G. et al. (1999) *Science 284*, 1348–1350. [5] Haisch K.E. et al. (2001) *Astrophys. J. 553*, L153–L156. [6] McKinnon W.B. (2006) in *Io After Galileo*, R.M.C. Lopes and J.R. Spencer, eds., Springer Praxis, 61-88. [7] Lissauer J.J. and D.J. Stevenson (2006) in *Protostars and Planets V*, Reipurth B. et al., Univ. Ariz. Press, in press. [8] Canup R.M., and W.R. Ward (2002) *Astron. J. 124*, 3404-3423. [9] Canup R.M. and W.R. Ward (2006) *Nature 441*, 834-839. [10] McKinnon W.B. and M.E. Zolensky (2003) *Astrobiology 3*, 879–897. [11] Stevenson D.J. et al. (1986) in *Satellites*, J.A. Burns and M.S. Matthews, eds., Univ. Ariz. Press, 39–88. [12] Stewart S.T. and T.J. Ahrens (2003) *Geophys. Res. Lett. 30(6)*, 65. [13] McKinnon W.B. (2006) *LPS XXXVII,* Abstract #2444. [14] McKinnon W.B. and E.M. Parmentier (1986) in *Satellites*, J.A. Burns and M.S. Matthews, eds., Univ. Ariz. Press, 718–763. [15] Showman A.P. and R. Malhotra (1997) *Icarus 127*, 93–111. [16] Peale S.J. and M.H. Lee (2002) *Science*, *298*, 593–597. [17] Lodders K. (2003) *Astrophys. J. 591*, 1220-1247. [18] McKinnon W.B. (2003) *LPS XXXIV*, Abstract #2104. [19] McKinnon W.B. (2004) *LPS XXXV*, Abstract #2137. [20] Gaetani G.A. and Grove T.L. (1999) *EPSL*, *169*, 147-163. [21] Bruhn N. et al. (2000) *Nature 403*, 883–886. [22] Scott H. et al. (2002) *Earth Planet. Sci. Lett. 203*, 399-412.

WATER ON MARS: BEHAVIOR OF H_2O DURING ACCRETION AND EARLY PLANETARY DIFFERENCIATION. E. Médard and T. L. Grove, Department of Earth, Atmospheric and Planetary Sciences, Massachusetts Institute of Technology, Cambridge MA 02139, USA (emedard@mit.edu; tlgrove@mit.edu).

Introduction: Recent evidence from Ceres, a small proto-planet orbiting in the asteroid belt, confirmed that water-rich planetary bodies were in existence during the early evolution of the Solar System [1,2]. The formation of water-rich versus dry bodies is likely a complex function of initial amount of water in the planetesimals, timing of accretion, and concentration of short-lived radioactive isotopes [3]. The existence of water-rich planetesimals and small-protoplanets in the inner Solar System allows reexamination of the hypotheses for the incorporation of H_2O into planets.

In the following, we investigate the consequences of a "wet accretion" scenario for the planet Mars, by comparing experimentally determined hydrous phase relations [4, Fig. 1] and thermal models of planetary evolution. There are two main reason to focus on Mars: (1) Mars formed farther from the Sun, and accreted from a chondritic mix that is richer in volatile elements than for other terrestrial planets [5]. (2) The size of Mars is almost identical to the typical size of a proto-planet just before the giant impact stage [6], suggesting that Mars may have escaped the formation of a planet-scale magma ocean that obliterated most of the signature of early accretion and differentiation processes on the Earth.

We propose that an early hydrous melting event occurred during the accretion process. This melting event profoundly differentiated the Martian mantle and removed H_2O from the planet's interior. Water has a strong effect on melting temperatures and mantle viscosity, and the presence of water will accelerate the differenciation process, in agreement with the evidence that Mars differenciated into atmosphere, mantle and core at a very early stage [7].

Thermal model: Abundant heat sources (accretion energy, radioactive decay of long and short-lived isotopes, core formation, etc.) insure that the planet would be progressively heated throughout the accretion process. Existing models of the thermal evolution of planets result in the same shape for the thermal profile of the planet: colder at the surface and in the center, with a temperature maximum closer to the surface than to the center [e.g., 10, 11, 12, 13]. All the models also show a progressive increase in temperature with time. Figure 2 is based on the model [13], which assumes that heating is exclusively caused by accretion energy and neglects the effects of decay of short-lived isotopes, core formation and heat transport by convection. Calculations using different models result in a qualitatively similar evolution, although slightly different amounts of melting and different amounts of H_2O stored in the planetary interior have been obtained.

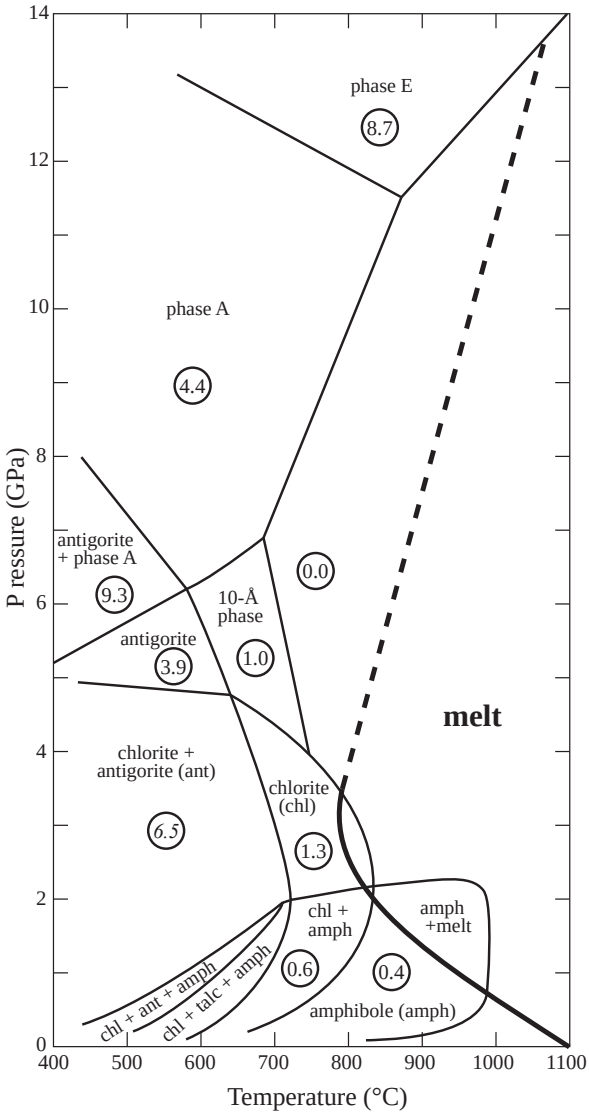

Figure 1. Water-saturated phase relations of a primitive mantle + crust Martian composition [8]. The hypothetical high-pressure solidus (dashed curve) is estimated from [9]. Circled numbers are estimated total water contents bound in hydrous phases, calculated from phase proportions and water content in hydrous phases. Figure from [4].

Fate of H_2O during accretion: During accretion, H_2O would be preserved in the hydrous minerals of chondrites which would remain stable until about 30 % of the mass of the planet (70% of the final radius) had accreted in a rapid accretion process (Fig. 2).

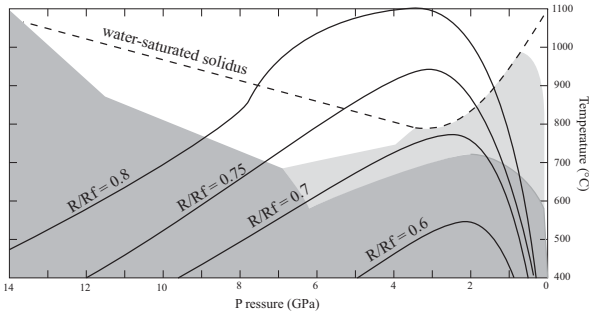

Figure 2. Thermal model of planetary accretion [13] compared to experimentally derived phase diagram for a wet Martian composition (Fig. 1). Different shades of gray represent the amount of water that can be bound in hydrous silicates: dark gray, ≥ 4 wt%, light gray 0.4-1.3 wt%, white, no stable hydrous phase. The dashed line is the water-saturated solidus, i.e., the low-temperature boundary of the melting region. Thin black lines are thermal profiles at different stages of planetary growth, when the planetary radius R was 0.6, 0.7, 0.75, and 0.8 times its final radius Rf. Major dehydration and degassing occur when the planet reached about 70% of its final radius (30% of its final mass). Figure from [4].

As accretion continued, interior temperature would increase (Figure 2) until it passes a series of dehydration and melting reactions. Dehydration in the deeper parts of the planet would lead to flux melting in the shallower parts. Planetary differenciation could thus start very early, even before the end of accretion.

The innermost part of the planet would remain undegassed during accretion (Fig. 3), and contains H_2O stored in buried hydrous silicates. A feature of all thermal models of planetary evolution is that the inside of the planet heats up only after or during the latest stages of accretion, as a result of core formation and heating by long-lived radioactive isotopes [14]. Large amounts of H_2O could thus be transferred into "nominally anhydrous silicates" in the deep mantle, and might even be incorporated into the core [15]. Using model [13], the maximum amount of H_2O that may be stored inside the planet is about 0.4 wt% of the total mass of the planet. Later degassing of this deep reservoir could trigger more fluxed melting of the external parts of the planet. This late flux melting would produce a proto-crust of basaltic andesite similar to that found in terrestrial subduction zone settings. Water will also be incorporated into convection cycles, reducing the viscosity, and accelerating the early differentiation of the planet [16]

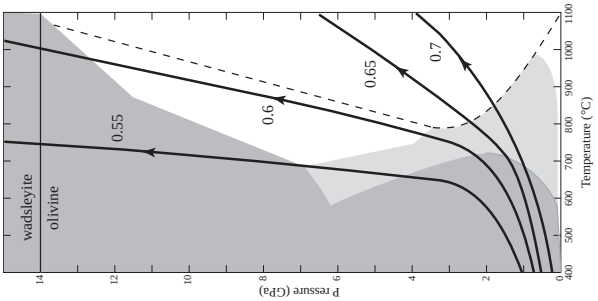

Figure 3. Calculated pressure-temperature paths for accreted material according to the model [13]. Numbers on the curves refer to the time when the material accreted, expressed in fraction of the final radius R/Rf. Material accreted before the planet reached 0.55 times its final radius (i.e. about 17% of its final mass) does not dehydrate, and water is transferred into the wadsleyite stability field, where it can be stored in "nominally anhydrous" minerals. Figure from [4].

References: [1] McCord T.B. and Sotin Ch. (2005) *JGR, 110,* E05009 [2] Thomas P.C. et al. (2005) *Nature, 437,* 1-3 [3] McCord T.B. et al. (2006) *Eos, 87-10*, 105-109 [4] Médard E. and Grove T.L. *JGR, E002742, in press* [5] Dreibus G. and Wänke H. (1985) *Meteoritics, 20,* 367-381 [6] Lunine J.I. et al. (2003) *Icarus, 165*, 1-8 [7] Folley C.N. et al. (2005) *GCA, 69*, 4557-4571 [8] Dreibus G. and Wänke H. (1984) *27th Int. Geol. Congress, 11*, 1-20 [9] Kawamoto T. and Holloway J.R. (1997) *Science, 276*, 240-243 [10] Kaula W.M. (1979) *JGR, 84,* 999-1008 [11] Coradini A.C. et al. (1983) *Phys. Earth Planet. Int., 31*, 145-160 [12] Abe Y. and Matsui T. (1986) *Proc. 17th Lunar Planet. Sci. Conf.,* E291-E302. [13] Senshu H. et al. (2002) *JGR E, 107,* 5118. [14] Hauck S.A.I. and Phillips R.J. (2002) *JGR, 107,* E75052 [15] Okuchi T (1997) *Science, 278,* 1781-1784. [16] Solomon S.C. et al. (2005) LPSC XXXVI, Abstract #1689

A NUMERICAL MODEL FOR NI PARTITIONING IN THE TERRESTRIAL MAGMA OCEAN. H. J. Melosh[1,2] and D. C. Rubie[1]. [1]Bayerisches Geoinstitut, Universität Bayreuth, 95440 Bayreuth, Germany. [2]Lunar and Planetary Lab, University of Arizona, Tucson AZ 85721. (jmelosh@lpl.arizona.edu).

Introduction: The partition of siderophile elements between a silicate liquid and a metal phase played an important role in establishing the observed siderophile element abundance in the Earth's present mantle. Current models of the Earth's formation recognize the importance of large impacts in the early history of the planet, and the fact that such impacts lead inevitably to the production of large volumes of melt [1, 2]. The formation and evolution of such "magma oceans" has become a standard part of the discussion of the early history of the Earth as well as the other terrestrial planets [3]. Understanding the abundances of the siderophile elements depends crucially on the thermodynamics of element partitioning between a silicate melt and metal phase as a function of temperature, pressure, oxygen fugacity and melt structure. Fortunately, many years of experimental study have produced a good understanding of how the partition coefficients of many elements depend on these parameters under realistic conditions [4]. However, chemistry is only part of the overall story: the mechanics of how the iron separates from the silicate strongly controls how much of the metal and silicate react together: If the iron sinks through the mantle in masses that are too large, little chemical partitioning will occur between the two phases. Even when the masses are smaller, as may occur for surface-tension-controlled droplets, the strong depth and temperature dependence of the partition coefficients is a major determinant of the final siderophile element abundances in the mantle [5].

Iron masses, in whatever form, do not sink quietly through a magma ocean: Their density variations drive vigorous convection currents that themselves tend to suspend and disperse the masses of iron. In addition, thermal convection may also stir the ocean [6]. A simple Stokes-flow model of iron settling cannot resolving the full complexity of iron segregation from a magma ocean and the resulting siderophile element partitioning. Although thermal convection in the planets has been intensively studied [7], much less is understood of the dynamic interactions between a convecting fluid and a second fluid that can separate from the first.

Numerical Method: In the research reported here, we began with a model for pyroclastic flows developed at Los Alamos [8]. This model is based on a computer code called KACHINA that incorporated the ability to compute the flow of two interpenetrating fluids that may move at any speed, ranging from slow subsonic to supersonic [9]. Although this particular code is now considered obsolete at Los Alamos, it was reborn later as KFIX [10]. The code is fully implicit, solving a pressure and mass balance constraint with velocities computed on a staggered mesh. Over the past year T. Goldin and HJM adapted this code to the problems of the interaction of planetary ejecta with the Earth's upper atmosphere [11] and magma ocean differentiation. We added subroutines to implement chemical exchange of trace chemical species (Ni in this case) between liquid magma and molten iron, following the scheme of Rubie et al. [5]. The magma equation of state is based on komatiite liquid [12], while the equation of state for the iron is derived from shock wave measurements on iron [13]. Partition coefficients are from Righter and Drake [14].

Computational Model: A computational mesh was constructed measuring 1,000 km deep and 1,000 km wide. Iron metal, in weight ratio of 0.37:1 of silicate, was uniformly distributed as 1 cm diameter droplets throughout the mesh at the beginning of the computation. The magma viscosity is taken to be 0.01 Pa-s as a rough average of the observed complex viscosity variation [15]. The initial concentration of Ni in the iron is 2.27 wt% and in the silicate 42 ppm. Initial temperatures are uniform at 2,000 K. This is thus a highly stable configuration from the point of view of thermal convection: an adiabatic temperature profile might have been a more realistic choice. In our initial runs the resolution is very coarse: only 10 x 10 computational cells. Considerable refinement is planned in the near future. Nevertheless, a number of prominent features can be readily observed.

Results: The most obvious feature is that, although the droplets initially began to fall in an orderly array at the Stokes velocity of about 0.3 m/sec, after no more than a few hours irregularities develop, creating compositional density currents that quickly dominate the flow. These currents reach up to 50 m/sec and completely overwhelm thermal convection. The falling droplets are swept upwards and downwards by this flow as they continue to settle with respect to the fluid. The net result of this vigorous motion is adiabatic chilling of the upper part of the mesh and heating of the lower mesh. These currents continue to stir the magma ocean as the droplets separate, slowly converting their gravitational potential energy to heat and warming the lower part of the ocean. Nevertheless, over a period of months the lower part of the magma ocean is strongly stirred by currents originating from compositional density differences. Thermal convection velocities in the upper, magma-dominated part of

the magma ocean reach about 7 m/sec, small compared to those driven by compositional convection.

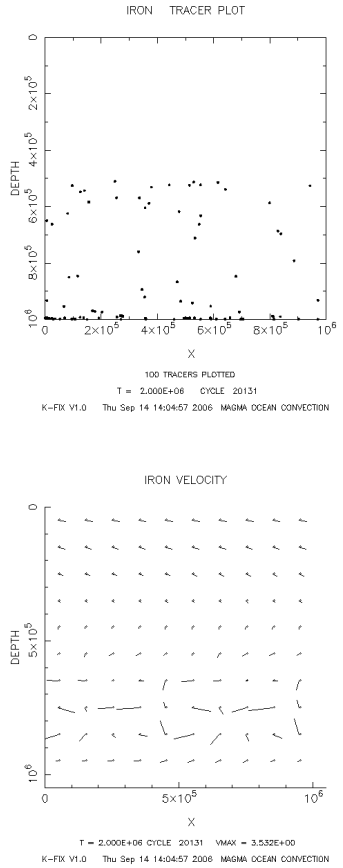

Figure 1. Iron droplet tracer particles showing the distribution and velocity of iron after about 23 days of settling. Note the high velocities are confined to the region containing the iron tracer particles.

Within about half a year, in this low-resolution model, most of the iron has settled to the bottom of the magma ocean. At this time, the average Ni concentration in the separated iron divided by that in the silicate magma is 15, in good agreement with Model 2 of [5] for a 1000 km deep magma ocean. Figure 1 shows a snapshot of the iron tracer particle locations and velocities 23 days after the beginning of the computation. About half of the iron has fallen out at this stage.

Many more runs, at higher resolution, are planned with this code and the results will be reported at the meeting.

References: [1] Melosh, H.J. in *Origin of the Earth* (eds. Jones, J.H. & Newsom, H.E.) 69 (Oxford University Press, New York, 1990). [2] Tonks, W.B. & Melosh, H.J. (1993) *J. Geophy. Res.* **98**, 5319. [3] Solomatov, V.S. in *Origin of the Earth and Moon* (eds. Canup, R.M. & Righter, K.) 323 (U. of Arizona Press, Tucson, 2000). [4] Wade, J. & Wood, B.J. (2005) *Earth Planet. Sci. Lett.* **236**, 78. [5] Rubie, D.C., Melosh, H.J., Reid, J.E., Liebske, C. & Righter, K. (2003) *Earth Planet. Sci. Lett.* **205**, 239. [6] Tonks, W.B. & Melosh, H.J. in *Origin of the Earth* (eds. Jones, J.H. & Newsom, H.E.) 151 (Oxford University Press, New York, 1990). [7] Schubert, G., Turcotte, D.L. & Olson, P. *Mantle Convection in the Earth and Planets* 1-940 (Cambridge U. Press, 2001). [8] Valentine, G.A. & Wohletz, K.H. (1989) *J. Geophys. Res.* **94**, 1867. [9] Harlow, F.H. & Amsden, A.A. (1975) *J. Comp. Phys.* **17**, 19. [10] Rivard, W.C. & Torrey, M.D. *K-FIX: A computer program for transient, two-dimensional, two-fluid flow* 1-125 (LANL, Los Alamos, 1977). [11] Goldin, T.J. & Melosh, H.J. (2006) *Meteoritics and Planetary Science* **Abstract# 5073**, [12] Miller, G.H., Stolper, E.M. & Ahrens, T.J. (1991) *J. Geophys. Res.* **96**, 11831. [13] Anderson & Ahrens, T.J. (1994) *J. Geophys. Res.* **99**, 4273. [14] Righter, K. & Drake, M.J. (1999) *Earth Planet. Sci. Lett.* **171**, 383. [15] Liebske, C. & al., e. (2005) *Earth Planet. Sci. Lett.* **240**, 589.

NEW, GEOPHYSICALLY-CONSTRAINED MARTIAN MANTLE COMPOSITIONS. M.E. Minitti[1], Y. Fei[2] and C.M. Bertka[3], [1]Center for Meteorite Studies, School of Earth and Space Exploration, Arizona State University, Tempe, AZ, 85287-1404 (minitti@asu.edu), [2]Geophysical Laboratory, Carnegie Institution of Washington, Washington, DC, 20015, [3]Directorate for Science and Policy Programs, AAAS, Washington, DC, 20005.

Introduction: The history of Martian accretion and differentiation, and the evolution of igneous activity through time, is imprinted on the compositions of the mantle and igneous crustal lithologies of Mars. ever-expanding sources of data exist to provide insight into Martian crustal lithologies; The Martian meteorites embody a thoroughly-studied collection of Martian igneous crustal lithologies that has been utilized to gain insight into the Martian interior and its differentiation history [e.g. 1,2]. The detail in which their chemistries and mineralogies are understood, however, stands in contrast to their lack of geologic context. The remote sensing data obtained by the Mars Global Surveyor Thermal Emission Spectrometer (MGS-TES) reveal the widespread presence of crustal lithologies on the Martian surface complementary to the Martian meteorites [3]. Whereas TES mineralogies, and chemistries derived from these mineralogies [e.g., 4], are known with less precision than those of the Martian meteorites, the TES data offer a global view of crustal mineralogy and derived chemistry with the geologic context that the Martian meteorites lack. The Mars Exploration Rover (MER) missions have directly measured igneous rocks that show affinities toward the Martian meteorites and the TES lithologies [e.g. 5,6] and thus potentially bridge the seemingly disparate Martian meteorite and TES datasets.

Understanding the connection between the composition and mineralogy of Martian igneous materials and the accretion and differentiation of Mars requires investigation of feasible Martian interior compositions. The most popular model for Martian mantle and core compositions was created by [1]. They derived Martian mantle and core compositions by linking element abundance and ratio data from the Martian meteorites to C1 chondrite compositions. Exploration of melting the mantle composition established by [1] (hereafter referred to as DW mantle) has met with mixed success in reproducing Martian igneous lithologies. Recently, partial melting (~20%) of a DW mantle was shown to yield melts with bulk compositions like those of the picritic basalts found at Gusev [7]. However, [8] could not derive melts equivalent to Martian meteorite parent magmas by melting of a DW mantle analog. Recent geophysical observations have further underscored issues with the DW mantle. The Martian moment of inertia, precisely determined by Mars Pathfinder [9] and refined by [10], and the crustal thickness, more tightly constrained by gravity and topography measurements from MGS [11], cannot be reproduced by calculations which utilize the mineralogical and density profile of Mars with a C1 bulk composition regardless of the assumed core composition [12,13]. Thus, removal of the C1 chondrite bulk composition criterion of [1] for Mars is necessary.

[12] demonstrate that moment of inertia and crustal thickness, despite their current uncertainties, place surprisingly powerful constraints on the composition of the Martian interior. The moment of inertia (I=0.364-0.365 [9,10] and crustal thickness (~50 km [11]) data dictate that for a core composition of Fe-14 wt.% S, Mars should have a bulk Fe/Si of ~1.32, a bulk Fe (wt.%) of ~23.10 [13] and a mantle with Mg# between ~74-78 [12]. Varying the core composition from pure Fe to pure FeS only expands the allowable range of mantle Mg# to between ~73-79 [12]. These data conclusively demonstrate that the Martian mantle has more Fe than the terrestrial mantle (Mg# ≈ 89-90; e.g., 14]. Calculations aimed at establishing bulk Martian mantle compositions with geophysically-permitted mantle Mg#, bulk Fe/Si and bulk Fe (wt.%) determined that these parameters could only be met through the accretion of Mars from combinations of chondritic meteorites [15].

New Mantle Compositions: Given the evidence that mixtures of chondritic meteorites are necessary to produce a geophysically-feasible bulk Martian mantle, we surveyed the compositions of candidate mantles using a calculation that mixes pairs of chondrites in proportions that result in a bulk composition with geophysically-permitted Fe/Si and Fe (wt.%) values. The inputs to the calculation are the bulk compositions of carbonaceous (C1, CM, CO and CV), ordinary (H, L and LL) and enstatite (EH and EL) chondrites [16] and the bulk planet Fe/Si and Fe (wt.%), which are uniquely defined by the moment of inertia (I=0.364-0.365; [9,10]) and a selected core composition (Table 1). Core compositions were chosen to cover the full range of possibilities; the Fe + 14 wt.% S core is the

Table 1: Martian compositional parameters dictated by I = 0.364-0.365 [12,13]

Core composition	Bulk Fe (wt.%)	Bulk Fe/Si
Fe	24.07	1.337
Fe + 14 wt.% S	23.10	1.319
FeS (36.5 wt.% S)	24.20	1.495

preferred core model of [1]. Of the nine chondrites to choose from, we selected endmember pairs whose bulk Fe/Si and Fe wt.% values bracketed the target Fe/Si and Fe wt% values for each core composition (Table 1). This resulted in 54 calculations (18 pairs of chondrites for each core composition). The next step of the calculation involved dividing the bulk composition resulting from the mixing calculation into mantle and core components using the assumptions that Fe/Mn of the Martian meteorites is representative of Fe/Mn of the Martian mantle and that the Martian core contains no Mn [1]. This step permitted calculation of the Mg# of the resulting mantle. Three metrics were then employed to evaluate the appropriateness of the calculated bulk compositions. First, because the calculation was not forced to result in mixture totals of 100, compositions were rejected on the basis of non-physical proportions of chondrites. Second, bulk compositions that did not yield bulk Fe/Si and Fe (wt.%) values appropriate for the selected core composition of the given calculation were discarded. Third, the derived mantle Mg# for each bulk composition was compared to the geophysically-allowed range of mantle Mg# (73-79 [12]) and mantles with Mg# values outside this range were rejected. The three metrics reduced the number of candidate mantle compositions from 54 to five.

Table 2: Selected Martian mantle compositions relative to previously studied compositions

	CM+L, Fe+S (14 wt%)	**H+L, Fe**	**DW[1]**	**A & D (2005)[2]**
SiO_2	46.86	47.61	44.5	47.0
Al_2O_3	3.14	2.78	3.0	2.68
MgO	30.70	29.99	30.2	30.5
FeO	15.05	15.55	17.9	13.3
CaO	2.50	2.24	2.5	2.1
Na_2O	0.35	0.46	0.5	1.12
P_2O_5	0.29	0.28	0.2	0.32
MnO	0.39	0.40	0.5	0.41
Cr_2O_3	0.70	0.69	0.8	0.66
Chondrite proportions	42:55	34:67	na	na
Bulk Fe (wt.%)	23.10	24.07	27.8	27.34
Bulk Fe/Si	1.34	1.31	1.71	1.63
Mantle Mg#	78.4	77.5	75.0	80.3
Modal mineralogy				
Olivine	37.1	32.8	48.1	31.6
Opx	39.5	46.3	29.0	48.1
Cpx	10.1	9.1	10.0	8.7
Garnet	13.3	11.8	12.9	11.6

[1]Bulk mantle comp. of Dreibus and Wänke (1985)

[2]Bulk mantle composition of Agee and Draper (2005)

na: not applicable

All five candidates are SiO_2-enriched and have higher proportions of modal orthopyroxene than the DW mantle and have intermediate Mg# relative to the mantles of [1] and [AD]. Because experimentation on five different mantle compositions is prohibitive, we selected two candidate compositions (CM+L, Fe-14 wt.% S core and H+L, Fe core; Table 2) that best represent the compositional and modal mineralogy range delineated by the five candidates. The selected compositions also permit testing of mantles associated with two separate core compositions.

Future Work: We will synthesize the two calculated mantle compositions and systematically study their mineralogy and melt compositions in primitive and depleted states under anhydrous and hydrous conditions. Depleted mantle melting is particularly interesting because proposed Martian magma ocean products have been successful in producing melts parental to the Martian meteorites [e.g. 17,18]. Success or failure of a depleted bulk mantle in producing magmas parental to Martian crustal lithologies could determine if a magma ocean is a necessary step in the evolution of the Martian mantle and crust. Through these experiments, we hope to constrain the conditions of Martian meteorite, TES and MER lithology formation including source region composition, source region depth, degree of melting and the potential role of water.

References: [1] G. Dreibus and H. Wänke (1985) *Meteoritics*, 20, 367-382. [2] D.C. Lee and A.N. Halliday (1997) *Nature*, 388, 854-857. [3] Bandfield et al. (2000) *Science*, 287, 1626-1630. [4] Hamilton et al. (2001) *JGR*, 106, 14733-14746. [5] H.Y. McSween, Jr. et al. (2004) *Science*, 305, 842-845. [6] H.Y. McSween, Jr., K.A. Milam and the Athena Science Team, *LPSC XXXVI*, #1202. [7] A.G. Monders et al. (2005) *LPSC XXXVI*, #2069. [8] C.M. Bertka and J.R. Holloway (1987) *PLPSC*, 18, 723-739. [9] W.M. Folkner et al. (1997) *Science*, 278, 1749-1752. [10] F. Sohl et al. (2005) *JGR*, 110, E12008, doi:10.1029/2005JE002520. [11] M.T. Zuber et al. (2000) *Science*, 287, 1788-1793. [12] C.M. Bertka and Y. Fei (1998a) *EPSL*, 157, 79-88 [13] C.M. Bertka and Y. Fei (1998b) *Science*, 281, 1838-1840. [14] A.E. Ringwood (1979) *Origin of the earth and moon*. [15] L. Gilpin et al. (2001) *LPSC XXXII*, #1717. [16] J.T. Wasson and G.W. Kallemeyn (1988) *Phil. Trans. Royal Soc. London, Series A*, 325, 535-544. [17] C.B. Agee and D.S. Draper (2005) *LPSC XXXVI*, #1434. [18] L.T. Elkins-Tanton et al. (2003) *MAPS*, 38, 1753-1771.

IMAPCT GROWTH IN LIGHT ELEMENTAL CHANGE AT EARLY PLANETARY FORMATION.

Y. Miura, Inst. Earth Sci., Graduate School of Sci. & Eng., Yamaguchi University, Yoshida 1677-1, Yamaguchi, 753-8512, Japan, yasmiura@yamaguchi-u.ac.jp

Introduction: In order to analyze change of light elements by "impact growth" (*i.e.* elemental change by impact process), a carbon element is selected before and after impact process because other light elements of hydrogen, oxygen and nitrogen show strong and irregular difference at element abundances among Universe, the Sun, meteorite and crustal rocks of the Earth [1]. Elemental abundances after impacts at early planetary formation are considered to be those of Universe and the Sun (as those before impacts) and of carbonaceous meteorites, crustal rocks and sea water of the Earth (as those after impact growth). The main purpose of the paper is to elucidate carbon change in impact process at early formation of the planets, together with other light elements.

Hydrogen and oxygen abundances: Hydrogen and oxygen elements reveal considerable change in the Solar System (Fig.1). In fact, elemental abundance of hydrogen is decreased from Universe and the Sun (*i.e.* 75% by weight) to planetary bodies of carbonaceous meteorite (2.4%) and crustal rocks of the Earth (0.15%). Oxygen shows considerable increase from Universe and the Sun (0.9% to 1.0%) to carbonaceous meteorite (41%) and crustal rocks of the Earth (46%) [1]. The elemental abundances suggest that light elements of hydrogen and oxygen are easily evaporated and escaped from impact site during impact process. These light elements are rich at outer planets of the Solar System after early planetary formation due to heavy impact process, and easily concentrated at living species (including human activity) as short term circulation of elements finally [2, 3, 4].

Carbon and nitrogen abundances: Carbon element shows similar abundances among Universe (0.5% by weight), the Sun (0.3%) and crystal rocks of the Earth (0.18%), though nitrogen shows strong decrease in crystal rocks of the Earth (Fig.1). Both elements are strongly rich in living species (including human activity) as short term circulation of elements [2, 3, 4, 5, 6]. In this sense, living species (including human activity) on the Earth planet can be explained as strong concentration of light elements as elemental cycles, compared with other places of universe, the Sun and meteorite asteroids. If there is no such carbon concentrated process, it is very difficult to form and found any type of carbon-bearing life materials on the Earth. In fact, oxygen and hydrogen are richer in water of the Earth (ca.86% and 11%, respectively) than human bodies (ca. 61% and 10%, respectively; Fig.1). On the other hand, carbon and nitrogen are exceedingly richer in human bodies (ca.23% and 2.6%, respectively) than crustal rocks (ca.0.18% and 20ppm by weight, respectively) and water of the Earth planet (28ppm and 20ppm by weight, respectively; Fig.1). Therefore, impact process is significant for elemental concentration especially in early planetary differentiation.

Volcanism and impact processes in elemental concentration: At early planetary formation, impacts by planetary dusts and asteroids-sized bodies are significant process of elemental concentration. However, volcanism which is produced by impacts (at early stage) or quakes in underground (at later stage of planetary bodies) is not a process to elemental circulation and concentration at early stage of planetary formation. On the present planet of the Earth, volcanism is a process to drive elemental cycle from solid to vapor or liquid at subduction zones of active Earth planet. In this sense, impact process is considered to be elemental circulation from rock to vapor on surface of planets, satellites and asteroids.

Breaking relicts of carbon cycle on the Earth: As carbon element shows similar abundances before and after impacts [1, 2, 3, 4, 5, 6], carbon is considered to be strong indicator of elemental circulation during impact growth process. If elemental circulation is complete, all light elements should be circulated. Elemental abundances can be checked only some observed, measured and calculated data so far [1]. Although hydrogen and oxygen are easily moved to outer planets of the Solar System, carbon can be checked even in local system during impact process. In this sense, carbon-rich rocks of coal, oil, natural gas and limestone formed at old age (for example, Akiyoshidai Plateau, Japan [2, 3, 6]) are considered to be breaking relicts of complete carbon cycles on Earth [3, 4, 5, 6]. If carbon cycle is complete, we cannot find any older rocks of carbon-bearing materials. Therefore, abrupt event of active water planet of the Earth to store underground by extraterrestrial impact event should be significant to explain existence of these carbon-rich rocks on present active Earth. The breaking process of carbon-bearing rocks on active planet of the Earth can be used to check whether there is water or carbon-bearing sedimentation on planetary body at impact growth or not as follows. When there is complete circulation system among air, water and rock, we can use it in active Earth planet, but cannot use the breaking process in the Mercury, Moon, Asteroids, and at least present Mars and Venus.

Carbon at Asteroids of carbonaceous chondrites: Oxygen and hydrogen elements are richer in carbonaceous chondrites (*i.e.* 41% and 2.4% , respectively), though carbon and nitrogen is minor abundances (*i.e.* 1.5% and 0.14%, respectively; Fig.1). This suggests that complete carbon cycles at three states of air, water and solid are not enough at asteroid surface, especially nitrogen to make complete living materials which is so poor at airless asteroids. However, elemental abundances of carbon and nitrogen in carbonaceous meteorite are the most abundant among Universe, the Sun, and water and crustal rocks of the Earth [1]. This indicates that carbon and nitrogen which are important for living species as

short term cycle should be considered to be transported from carbonaceous meteorites of asteroids which are ca. 5 times and 70 times rivher than those of crustal rocks of the Earth.

Summary: The results in this paper are summarized as follows.

1) Impact growth process can be analyzed by elemental abundances of light elements of hydrogen, oxygen, carbon and nitrogen at early planetary differentiation.

2) Carbon is considered to be strong indicator of elemental cycle during impact process.

3) Breaking process of carbon by impacts can be found as carbon-bearing rocks of water planet of the Earth.

4) Carbon and nitrogen formed during impact process on the Solar System are transported mainly from present carbonaceous asteroids which make acceleration to form short term carbon cycle of active process on the water planet of the Earth.

References:

[1] Winter M. (2006): *Periodic table web- elements* (Univ. Sheffield). http://www.webelement.com

[2] Miura Y. (2006): *Antarctic Meteorites* (NIPR, Tokyo), 73-74.

[3] Miura Y. (2006): *LPS XXXVII, abstract (LPI/ USRS, USA).* CD #2441.

[4] Miura Y. (2006): *2nd Hayabusa Symposium (Univ. Tokyo)*, 49-50.

[5] Miura Y. (2006): *Workshop on Spacecraft Reconnaissance of Asteroid and Comet Interiors* (LPI, USA). CD#3008.

[6] Miura Y. (2006): *ICEM2006 symposium abstract paper volume* (Yamaguchi University, Yamaguchi, Japan). 112-113.

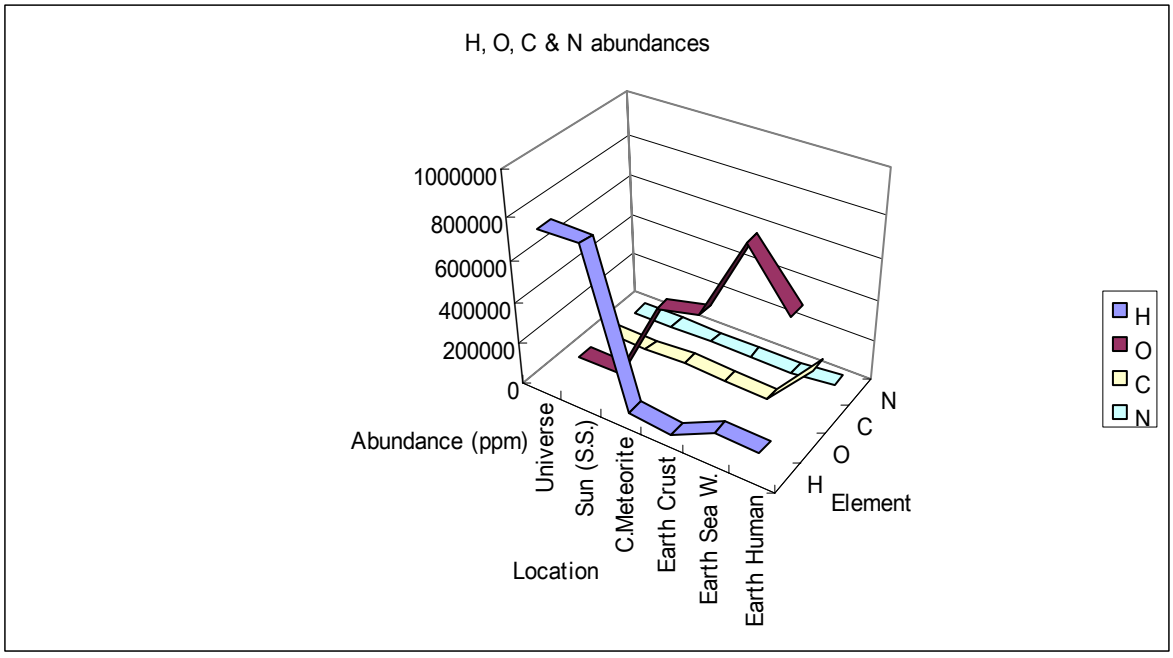

Fig.1. Carbon, hydrogen, oxygen and nitrogen elemental abundances at Universe, the Sun, carbonaceous meteorites, and crustal rocks, sea water, stream and human on the Earth planet [1, 2, 3, 4, 5, 6].

SEARCHING FOR NON-VESTOID BASALTIC ASTEROIDS Nicholas Moskovitz[1], Robert Jedicke[1], Mark Willman[1] and Eric Gaidos[2], [1]Institute for Astronomy, University of Hawaii, 2680 Woodlawn Drive, Honolulu, HI, 96822, nmosko@ifa.hawaii.edu. [2]Department of Geology and Geophysics, University of Hawaii, POST 701, Honolulu, HI, 96822.

Introduction: The presence of a basaltic surface on an asteroid is indicative of past partial melting. Partial melting and differentiation can occur if the internal temperature of a primordial asteroid or parent body rises above the solidus point of the constituent material. Possible sources for such a rise in temperature are the decay of radioactive isotopes, energy released during collisional accretion and various chemical processes such as serpentinization reactions. The complicated interplay of these heating processes with various cooling mechanisms such as fluid convection and thermal radiation have presumably contributed to the diversity of present day surface properties observed amongst the Main Belt asteroids. This work will provide observational constraints on the occurrence of asteroidal differentiation, which can in turn offer insight to the conditions and processes that have led to the evolution of small bodies in the Solar System.

Main-Belt Asteroid Differentiation: Samples of collected iron meteorites reveal a fundamental paradox regarding differentiation in the Main Belt. These recovered meteorites represent the one-time presence of as many as 60 differentiated parent bodies [1]. However there are only two known occurrences of Main Belt differentiation: 4 Vesta and the dynamically associated Vestoid family [2] and 1459 Magnya which is dynamically dissociated from V-type asteroids and therefore counted as a separate occurrence of differentiation [3].

Additionally, the widespread occurrence of differentiation throughout the inner Solar System (all of the terrestrial planets and the Moon) suggests that this process was a common phenomenon in the early Solar System. The question that remains then is: are there undiscovered basaltic asteroids in the Main Belt that are not part of the Vestoid family or has some process like collisional resurfacing effectively altered their basaltic spectral signature?

Selecting Basaltic Asteroid Candidates: To answer this question we have begun an observational campaign to obtain spectra for dozens of Main Belt asteroids. The candidates for this program are chosen to maximize the potential for discovery of new basaltic asteroids. Targets are selected from the Sloan Digital Sky Survey (SDSS) Moving Object Catalog (MOC) [4] based on their *ugriz* colors and orbital parameters. The targets that achieve the highest priority for spectral follow-up are those that (1) have a photometric signature that is similar to the V-type asteroids and (2) are dynamically distinct from this family. Eight different *ugriz* color combinations as well as two principle component colors [5] are used to define the regions in color-color space occupied by the 1175 Vestoids in the MOC. Candidate non-Vestoid basaltic asteroids are those that meet the color selection criterion and lie outside of the range of orbital element phase space occupied by Vesta and the associated Vestoids. Candidates are then prioritized based on their D-parameter [5], i.e. the distance from Vesta in orbital element phase space. Figure 1 is a color-color plot of the Vestoids (red circles), other MOC objects (blue contours) and our basaltic asteroid candidates (black X's). Clearly the basaltic candidates have colors that are well correlated to those of the Vestoid population which itself is quite distinct from the S and C-types whose numbers dominate the MOC color data. Figure 2 is a plot of osculating orbital elements for the Vestoids, MOC objects and our basaltic candidates. The apparent overlap of some candidate asteroids with the Vestoid population is merely a projection effect along the unplotted orbital inclination axis.

Observations: Low-resolution spectroscopy of candidate asteroids is performed using the Echellette Spectrograph and Imager (ESI) on Keck II in order to unambiguously determine whether our targets have basaltic surfaces. The 0.4 – 1.0 micron wavelength coverage of this instrument is well suited to resolving both the 0.9 micron olivine/pyroxene absorption feature and the 0.5 – 0.7 micron slope that are signatures of a basaltic surface and thus that a given asteroid derives from a parent body that has experienced either partial melting or differentiation. ESI is operated in the Low-Dispersion prism mode with a 6 arc second slit. For the second semester of 2006, two nights were awarded to this project during which ~10 asteroids will be observed. The results of these observations will be presented. Specific asteroids included in these observations are 1998 UM21, 1999 ST116, 2002 TV237 and 1999 GG2.

This research is supported by NASA Terrestrial Planet Finder grant NNG04GL48G, P.I. E. Gaidos, NSF Planetary Astronomy grant AST04-07134, P.I. R. Jedicke and NASA GSRP grant 7228, P.I. E. Gaidos.

References: [1] Chabot N. L. and Haack H. (2006) in *Meteorites and the Early Solar System II*, eds. D. S. Lauretta and H. Y. McSween Jr. [2] McCord T. B. et al. (1970) *Science*, 168, 1445. [3] Lazzaro D. et al. (2000) *Science*, 288, 2033. [4] Ivezic Z. et al. (2002) in *Survey and Other Telescope Teechnologies and Discoveries*, eds. J. A. Tyson and S. Wolff. Proceedings of SPIE Vol. 4836. [5] Nesvorny D. et al. (2005) *Icarus*, 173, 132.

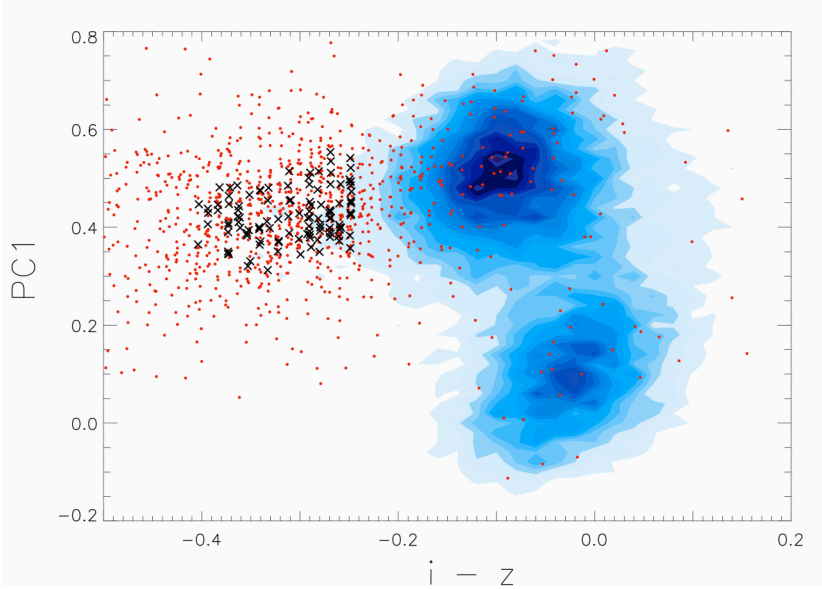

Figure 1 *i* - *z* versus PC1 color-color plot. PC1 refers to Principle Component 1 as parameterized by [5]. The blue contours are based on the SDSS MOC data and represent a two-dimensional histogram for the number of objects within a given color-color bin. The peaks of the S and C-type families are apparent. The colors of the 1175 Vesta-type asteroids that are included in the MOC are plotted as red circles. The 114 candidate basaltic asteroids to be targeted by this observing program are represented by the X's.

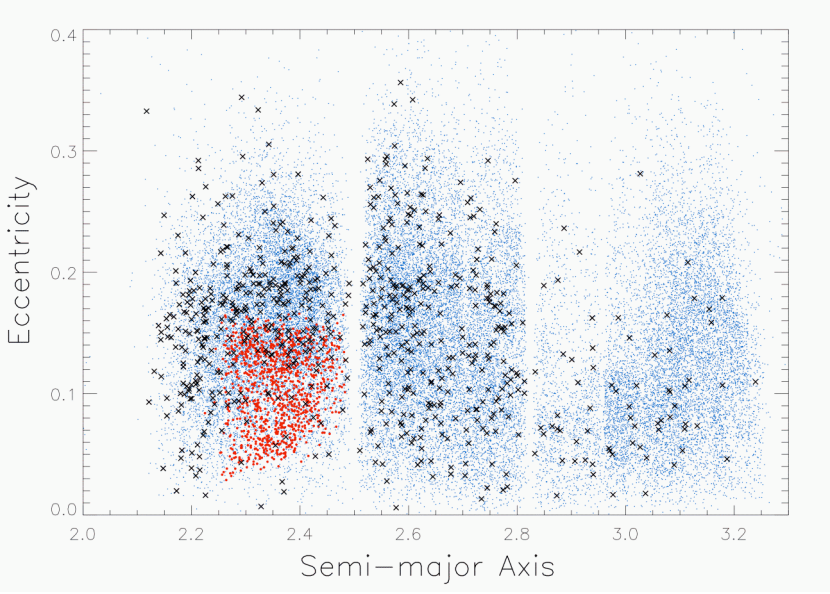

Figure 2 Osculating orbital elements of Vestoids (red circles), MOC objects (blue dots) and our basaltic candidates (black X's). The apparent overlap of some candidates with the Vestoids is due to projection along the unplotted orbital inclination axis. In fact these two populations lie in completely distinct regions of orbital element phase space.

Uranium in the Earth's Core? Metal-silicate partitioning of Uranium at High Pressure and Temperature and Highly Reducing Conditions.

V Rama Murthy, David S. Draper, and Carl B. Agee, Astromaterials Institute, University of New Mexico, Albuquerque, NM 87131. vrmurthy@unm.edu, david@draper.name, agee@unm.edu

Introduction: The presence of radioactive elements and consequent radiogenic heat production in Earth's metallic core has been the subject of many experimental and theoretical investigations (e.g., 1-12). The conventional wisdom is that K, U, and Th, the major radioactive heat producing elements in the earth, are strongly lithophile and hence would not partition into the core. However, it has become abundantly clear in recent years that the partitioning behavior of elements between metal and silicate is not invariant, but is affected by several variables such as, P, T, composition, oxygen fugacity etc. In that context, it has been recently shown that K can be present and act as a potential heat source in the core (1-5). We focus here on **uranium**, another important heat producing radioactive element in the Earth, and report on experiments that explore its presence and potential as a heat source in the core. A specific emphasis of this work is to study the partitioning behavior of U at highly reducing conditions in a magma ocean setting.

Experimental: We measured the partition coefficient of U, $D_U = U^{metal}/U^{silicate}$, between Fe-S-Si melts and molten enstatite chondrite run at ~4 log units below the iron-wüstite oxygen buffer and pressures between 3 and 8 GPa in a Walker-style multianvil press in the Astromaterials High Pressure Laboratory at the University of New Mexico. The starting materials consisted of mixtures of the EH enstatite chondrite Abee, reagent pure Fe, FeS, FeSi, and natural uraninite, ground under ethanol to a fine powder. Sample mixtures were contained in graphite capsules and run at super-liquidus temperatures (2200-2400°C) in castable-ceramic octahedra with alumina inner parts. Both metal and silicates were completely molten to simulate the liquid state of an early global magma ocean. All run products were analyzed by electron microprobe operating at 15 kV accelerating voltage and 20 nA beam current with counting times yielding uranium detection limits ~100 ppm. Mg was used to monitor silicate contamination in metal analyses. Typical run products consisted of fine quench textured silicate and two metallic liquids, one phase dominantly Fe-S rich, and the other phase dominantly Fe-Si (Fig 1). In many experiments, circular blebs of metal exsolved into sulfur rich and sulfur poor metallic liquids, the latter containing several wt. % Si.

Data and Discussion: D_U is in the range of 0.03-0.08 in our experiments. These values are significantly higher than those observed by Wheeler et al. (9). The reason for this difference is not clear at present, but may presumably be due to the highly reducing conditions of our experiments or due to differences in starting materials. We observe no systematic effect of pressure on D_U (Fig. 2), in agreement with the findings of Wheeler et al. (9) but in contrast with the data of Bao et al (12), who reported a strong pressure dependence.

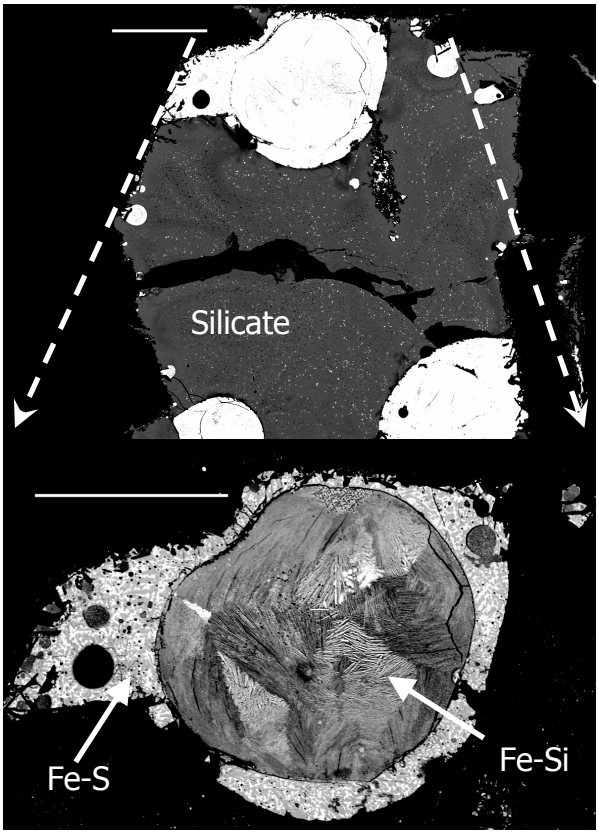

Fig. 1. Backscattered electron images of typical run product showing metal (bright) and silicate melts. Lower image is enlargement of topmost metal bleb from upper image. Dark blades are graphite crystals. Scale bars are 200 μm.

D_U is inversely correlated with Si in metallic liquid but shows a positive correlation with S, as observed by Wheeler et al. (9). In metal with little or no sulfur, D_U is lower by an order of magnitude or more. In the limited range of our measurements, 2200-2400°C, we did not observe any strong dependency of D_U on T, in agreement with Wheeler et al (9).

We note that U concentrations in metal-sulfide show no correlation with those of Ca, suggesting that U incorporation into the metal is not via the formation of CaS at these highly reducing conditions as was suggested by Furst et al. (10) and Murrell and Burnett (11). Nor does the U content of metal-sulfide have any discernible dependency on the O content of the metallic liquid. Thus, it appears that neither Ca nor O act as carriers or catalysts for entry of U into the metal sulfide. Rather, we suggest that the reaction $UO_2 + 2FeS = US_2 + 2FeO$ proceeds to the right at elevated P and T and highly reducing conditions, facilitating the incorporation of U in Fe-S liquids.

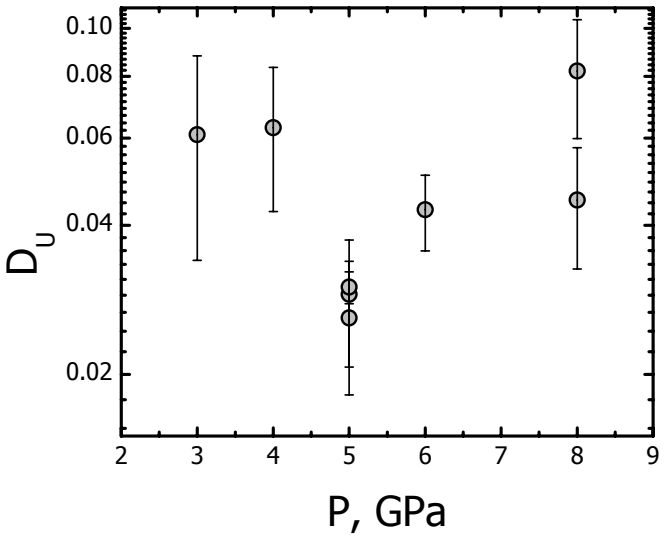

Fig. 2. D_U vs. pressure. Error bars are 2σ. Note absence of any pressure effect.

The potential effects of pressure and temperature on D_U need confirmation by further studies. If in fact there are no such effects and the behavior of D_U is not significantly changed at the much higher P and T relevant to magma ocean conditions, we estimate the U content of the core to be in the range of 1-2 ppb. The corresponding heat production capacity is 0.1-0.3 TW, which is only a small fraction of the estimated 6-12 TW total heat flux from the core (13). We conclude that under highly reducing conditions U exhibits distinct chalcophilic affinity and it is possible to incorporate U into the core under these conditions. However, the amount of U and hence its role as a radioactive heat source in the core is likely to be small unless D_U happens to be greatly increased at magma ocean pressures and temperatures.

References: [1] Gessmann C. K. and Wood B. J. (2002) *EPSL, 200,* 63-78. [2] V. Rama Murthy. et al. (2003) *Nature, 423,* 163-165. [3] Lee K. K. M. and Jeanloz R. (2003) *GRL, 30, 2212*. [4] Hirao N. et al. (2006) *GRL, 33,* L08303. [5] Bouhifd, M. A., et al. (2006) *PEPI* in press. [6] Chabot, N. L. and Drake, M. J., (1999) *EPSL*, 172, 323-335. [7] Bukowinski, M. S. T. (1976) *GRL,* 3, 491-503. [8] Lee K. K. M. et al. (2004) *GRL*, 31, doi: 10.1029/2004GL019839. [9] Wheeler, K. T. et al. (2006) *GCA*, 70, 1537-1547. [10] Furst, M. J., et al. (1982) *GRL,9, 41-44.*[11] Murrell, M. T. and Burnett, D. S., (1986) *JGR*, 91, 8126-8136. [12] Bao, X. et al. (2006). [13] Bufett, B. A., (2003) *Science,* 299, 1675-1677.